NASA TECHNICAL NOTE

NASA TN D-2419

NASA TN D-2419

A TWIN-GYRO ATTITUDE CONTROL SYSTEM FOR SPACE VEHICLES

by Jerry R. Havill and Jack W. Ratcliff

Ames Research Center

Moffett Field, Calif.

NATIONAL AERONAUTICS AND SPACE ADMINISTRATION • WASHINGTON, D. C. • AUGUST 1964

A TWIN-GYRO ATTITUDE CONTROL SYSTEM FOR SPACE VEHICLES

By Jerry R. Havill and Jack W. Ratcliff

Ames Research Center
Moffett Field, Calif.

NATIONAL AERONAUTICS AND SPACE ADMINISTRATION

For sale by the Office of Technical Services, Department of Commerce,
Washington, D.C. 20230 -- Price $1.00

A TWIN-GYRO ATTITUDE CONTROL SYSTEM FOR SPACE VEHICLES

By Jerry R. Havill and Jack W. Ratcliff

Ames Research Center
Moffett Field, Calif.

SUMMARY

This report describes the twin-gyro concept and the study of a three-axis attitude control system. Results of experimental data obtained from laboratory tests that used physical components are presented.

A twin-gyro controller consists of two counterrotating gyro elements arranged so that control torque is always directed about a single axis independent of gyro gimbal angle. This feature allows the use of large gimbal angles so that a major portion of the momentum stored in the gyros can be transferred to the vehicle without introducing cross-coupling torques.

The twin-gyro attitude control system uses three twin-gyro controllers to provide torques about three orthogonal vehicle axes. To study the control system experimentally it was mounted on a space vehicle simulator. The vehicle simulator had large values of inertia and was supported on a low-friction spherical air bearing.

The results of the experimental study, which are given in the report, show that a twin-gyro control system can stabilize a vehicle to precise attitudes (within 1 arc second) with good dynamic response. The system transfer function is derived and a comparison of the measured response with the calculated response shows that the system performance can be predicted analytically.

General theoretical equations of motion, derived for a single-degree-of-freedom gyro, a twin-gyro controller, and a three-axis twin-gyro attitude control system, are included as appendixes to the report.

INTRODUCTION

Some space flights require precise vehicle attitude control, and, depending upon the mission task, the requirements for pointing accuracy may impose very stringent specifications upon the control system. As examples, a high degree of rate stabilization may be demanded during navigational sightings for a manned space flight, and pointing accuracy within 1 arc second may be required for astronomical projects involving vehicle-fixed telescopes.

Several methods of generating torque for attitude stabilization have been studied at Ames Research Center. These include a system using reaction wheels

as reported in reference 1, a system using earth's magnetic field as reported in reference 2, and a system using three floated integrating rate gyros as reported in reference 3.

When a space vehicle is required to maintain a precise attitude with respect to inertial space, momentum exchange systems with proportional control become attractive. Of the two most commonly considered momentum exchange methods, the control-moment gyro provides a higher dynamic response than does the inertia wheel for a rotating element of given size.

Cross-coupling torques produced by a control system which uses a single gyro for each vehicle axis can be essentially eliminated by a twin-gyro control system. The twin-gyro concept consists in mounting two counterrotating wheels back to back. Their gimbals are driven through equal but opposite angles in order to nullify undesired components of angular momentum which introduce cross-coupling torques. Such a pair of gyros constitutes a controller capable of producing torque that is always directed about a single axis regardless of gimbal angles. This feature allows the use of large gimbal angles so that a major portion of the momentum stored in the gyros is available for transfer to the vehicle. It therefore has an advantage over a single-gyro controller which must be restricted in gimbal angle to minimize cross-coupling torques. The twin-gyro configuration has been described for use in a pitch damping system (ref. 4) and has been proposed for a local vertical sensor (ref. 5).

The research reported here is part of an investigation of the feasibility of stabilizing a space vehicle to precise attitudes (within 1 arc second) by use of a twin-gyro configuration of control-moment gyro torquers. Experimental data obtained from a space vehicle simulator stabilized about three axes has been presented in reference 6. The present report will show that the stabilized vehicle had good dynamic response and that this response can be predicted analytically.

DESCRIPTION OF CONTROL SYSTEM

A block diagram of one axis of the attitude control system is shown in figure 1 using the notation in appendix A. The attitude sensor produces a signal voltage proportional to the angular error between a vehicle axis (attitude) and a reference axis. This error signal, along with its integrated value, drives a twin-gyro controller whose precession torque is applied to the vehicle in the direction required to reduce the attitude error.

General theoretical equations of motion of a single-degree-of-freedom gyro, a twin-gyro controller, and a three-axis twin-gyro attitude control system are presented in appendixes B, C, and D, respectively. The block diagram of figure 1 corresponds to the theoretical transfer function derived in appendix D (eq. (D22)) with the addition of a filter time lag associated with the attitude error sensor and a compensating lead-lag network.

Twin-Gyro Controller

Figure 2 shows a twin-gyro controller wherein each gyro consists of a gyro element (wheel) spinning within a gimbal support. Each gimbal is pivoted to the controller frame about its gimbal axis which is normal to the gyro wheel spin axis. Notice that the direction of the net momentum change that results when the two gyro gimbals are rotated through equal and opposite angles from the gyro spin reference axis remains normal to the gyro spin reference axis and always along the momentum exchange axis, while the undesired components of momentum along the spin reference axis are cancelled. This cancellation eliminates the major source of cross-coupling torque inherent in single-gyro controllers and allows the twin-gyro gimbals to be driven through large angles (approaching 90°) so that essentially the entire angular momentum stored in the gyro elements may be transferred to the vehicle. In addition, the torque reactions from the gimbal drive motors are equal and opposite with cancellation taking place in the frame of the controller upon which both motors are mounted, thus eliminating a minor source of cross-coupling torque.

A block diagram of one twin-gyro controller with its gimbal position servo loops is shown in figure 3. Each gyro gimbal is provided with a position (angle) pickoff whose output voltage is a function of the gimbal angle. If the gimbal position feedback signal differs from the error signal input to the controller, the resulting difference signal drives the servomotor which torques the gimbal to reduce the position error. A tachometer generator provides gimbal rate feedback for stabilization of the gimbal servo. Note that the error signal input to gyro "b" has been inverted and that the two-position servo loops are otherwise identical so that the gimbal angles are maintained equal and opposite.

One of the twin-gyro controllers with its drive amplifier is shown in figure 4. As seen in this photograph the gimbal torquing motors are mounted on one end of each gimbal axle and the position feedback synchros are mounted on the opposite end of each gimbal axle. Each gyro element has a specified angular momentum of 55×10^{6} gm-cm^2/sec. The gimbals could be driven at a maximum rate of 1 radian/sec and the maximum torque available from each controller was 1.1×10^{3} dyne-cm or approximately 8 lb-ft. Three of these units were rigidly mounted on the vehicle.

The twin-gyro controllers were originally designed and constructed by Chance Vought Electronics under contract to NASA, Ames Research Center.

Signal Processor

When the twin-gyro controller is used for controlling the attitude of a vehicle, its gimbals must be driven at a rate proportional to attitude error to develop a control torque which is proportional to attitude error. Therefore, if the vehicle is to maintain attitude stability in the presence of

external disturbance torque, the controller gimbals must be driven by an integrated attitude error signal. This integration becomes necessary because gimbal position feedback is employed in the controller.

The purpose of the signal processor is to provide the required integrated error signal plus a proportional error signal. The signal processor also includes a lead-lag network which compensates for a time lag in the controller servo. These functions were generated by an analog computer for each of the three twin-gyro controllers.

Attitude Error Sensor

Attitude reference axes were established by means of two optical error sensors external to the vehicle and two point sources of light mounted on the vehicle. One sensor-source combination was used for pitch and yaw attitude errors and one for roll attitude errors. The roll attitude error sensor and light source are shown in figure 5. The sensor sensitivity was approximately 70 millivolts per arc second attitude error. The sensors were calibrated in increments of 5 arc seconds measured by an optical autocollimator which was used as the standard.

Vehicle

The vehicle simulator and associated laboratory apparatus are shown in the photograph of figure 5. The simulator, which was supported on a low-friction air bearing, was large enough to accommodate a man and had an overall weight of approximately 1800 kilograms (4000 lb).

The inertia values used in this investigation are presented in figure 6. This figure also indicates the location of the three twin-gyro controllers, and defines the orientation of the two light sources and associated attitude sensors which established the reference axes. The simulator axes were chosen to have the directions of the orthogonal set of unit vectors $\overline{E}_{V1}$, $\overline{E}_{V2}$, and $\overline{E}_{V3}$, hereafter referred to as the roll, pitch, and yaw axes, respectively.

Electrical power and signals between equipment on and off the simulator were transmitted through flexible wiring around the supporting air bearing. Since the simulator was restricted to rotations of only a few arc minutes about each axis, the wiring around the bearing produced no noticeable torques on the vehicle. The number of wires around the bearing was reduced by reversing the usual detector-source relationship, that is, by mounting the light sources (stars) on the vehicle. Since there was no requirement for a completely self-contained system aboard the vehicle, the attitude sensors, recording and display equipment, an analog computer used for signal processing, and the system control panel were all located external to the vehicle.

A cold-gas reaction jet system was installed on the vehicle for automatically returning each twin-gyro controller to its zero-momentum position ($\theta_c = 0$) whenever its gimbal angle exceeded a predetermined value ($\pm 60^\circ$).

Provisions were made for adjusting the center of mass as closely as possible to the center of rotation previous to each data run.

Controller Orientation

Consider now the orientation of the three twin-gyro controllers with respect to the vehicle. The three controller momentum exchange axes must be parallel to the vehicle body axes. The spin reference axis of each controller can be arbitrarily oriented in the plane perpendicular to its momentum exchange axis, since for the twin-gyro configuration no net angular momentum exists about the spin reference axis. If the gyro spin axes are "caged" (i.e., held in the zero gimbal angle position) then both gyros of a controller may be turned on or off during flight with, ideally, no disturbance torque reacting on the vehicle. This feature could be used to conserve power or to extend the lifetime of a mission in cases where the gyros are not required to be operating continuously.

Another mode of operation which may be of interest for certain missions involves using only three gyros (one from each controller) for vehicle control during portions of the mission not requiring the higher performance capabilities of the complete twin-gyro system. Such a mode of operation becomes feasible with the particular controller orientation shown in figure 7. Notice, for example, that the set of three "a" gyros is arranged so the angular momentum vectors form a closed triangle (zero net momentum) when the gimbal angles are zero and the three wheels contain equal angular momentum. Therefore, the set of three gyros, under the "caged" condition with no net momentum, could be turned on or off during flight without disturbing the vehicle if the three wheels accelerate or decelerate simultaneously. Since the twin-gyro system can be considered as two such three-gyro control systems, this particular controller orientation was used in the investigation to test this mode of operation. When sets of three "a" (or "b") gyros were turned on and off (always leaving at least three gyros in control), the resulting vehicle disturbance was negligible.

The visual interpretation of figure 7 may be facilitated by recognizing that the gimbal axes of the yaw controller, for example, lie in the plane defined by $\overline{E}_{V1}$ and $\overline{E}_{V2}$, so that the momentum exchange axis for the twin-gyro controller is parallel to the $\overline{E}_{V3}$ or vehicle yaw axis.

COMPARISON OF MEASURED AND ANALYTICAL RESULTS

The vehicle simulator described in the preceding section was assembled in the laboratory and tested to determine its dynamic characteristics and to

obtain experimental data from which to compute the system transfer function. The gains and compensation time constants were adjusted to achieve the best transient response in all axes.

A simultaneous step input to three axes produced the attitude response shown in figure 8. It can be seen that the control system was able to maintain the commanded attitude to within 1 arc second.

The analysis of appendix D shows that control torques generated by the ideal twin-gyro controller exist only about the desired control axis. This is shown in equation (D15), where it can be seen that $\bar{M}_{VZ}$, for example, is dependent on $\dot{\theta}_{CZ}$ but is independent of $\dot{\theta}_{CX}$ and $\dot{\theta}_{CY}$. It should be observed in equation (D15), however, that vehicle rates, ω_1 and ω_2, for example, cause a small cross-coupling torque about the z axis if nonzero values exist in θ_{CX} or θ_{CY}. The reason is that the controller gimbals are carried with the vehicle, and a gyroscopic coupling torque may be developed, as a result of vehicle rate, by a controller having a net angular momentum ($\theta_C \neq 0$).

The procedures used for obtaining the experimental data and for evaluating the yaw control system transfer function will now be described. The measured frequency response of the yaw-axis twin-gyro controller was used to determine its transfer function which was then combined with analytical data for the remainder of the yaw control system to produce the complete yaw-axis open-loop transfer function.

To measure the frequency response of the twin-gyro controller, sinusoidal input signals were introduced over the frequency range of 0.2 to 10 cycles per second and the gyro gimbal angles were recorded. Figure 9 shows the amplitude ratio and phase angle plotted as functions of frequency. A high-frequency resonance which occurred above 5 cycles per second was probably caused by mechanical compliance of the gimbal axle. The frequency response shown in figure 9 was used to determine an analytical expression for the transfer function of the twin-gyro controller:

$$\frac{\theta_C(s)}{E_C(s)} = \frac{8\times10^4}{(s + 5)(s + 80)(s + 0.1 + j34)(s + 0.1 - j34)}$$

The imaginary roots were factored from the second-order term $(s^2 + 0.2s + 34^2)$. Figure 10 shows how this transfer function was combined with the transfer function of the rest of the yaw control system to produce the over-all transfer function block diagram. A comparison with figure 1 shows that the vehicle rate feedback to the controller gyros is not included in figure 10. This feedback may be neglected because of the high gain used in the gimbal position loop compared to the gain in the vehicle rate loop.

The controller output torque, m_V, results from $2h\dot{\theta}_C \cos\theta_C$ which, for small angles, is approximated by the linear relation $m_V = 2h\dot{\theta}_C$. Hence, the Laplace transform is $M_V(s) = 2hs\theta_C(s)$, where h is the angular momentum of one gyro element, and the transfer function from gimbal angle to torque is $M_V(s)/\theta_C(s) = 1.1\times10^8 s$.

The over-all open-loop transfer function from e to e_s was

$$\frac{E_s(s)}{E(s)} = -\frac{4\times10^8(s+1)}{s^2(s+64)(s+80)(s+10)(s+0.1+j34)(s+0.1-j34)}$$

Figure 11 shows the root locus of the characteristic equation. The arrows indicate the direction in which the roots of the characteristic equation move as gain is increased. Their positions for the gain used in the experimental system are indicated by the solid dots on the locus. Once the roots from the root-locus plot are determined, it is possible to describe the closed-loop transfer function in factored form as

$$\frac{E_s(s)}{E_{in}(s)} = \frac{4\times10^8(s+1)}{(s+67)(s+78)(s+1.25)(s+3+j6)(s+3-j6)(s+0.1+j34)(s+0.1-j34)}$$

As a check on the validity of the derived transfer function, a plot of the corresponding calculated closed-loop frequency response was compared with the measured frequency response of the system. The close agreement indicated in figure 12 justifies the use of the derived transfer function as a good approximation of the system performance.

If a constant external torque, M_V, is applied to the vehicle, the twin-gyro controller will produce an equal and opposite torque, m_V, as a result of the static attitude "standoff" error. During application of unidirectional external torque, the gyro gimbal angles increase continuously until the operating range of the gyros is exceeded. The ability of the system to maintain attitude in the presence of external disturbance torque can be determined from the transfer function between M_V and θ_V of figure 10. This is indicated by

$$\frac{\theta_V(s)}{M_V(s)} = \frac{\dfrac{1.05\times10^{-11}}{s^2}}{1+\dfrac{1.05\times10^{-11}}{s^2}\dfrac{1.45\times10^5}{(s+10)}\dfrac{30(s+1)(s+5)}{s(s+64)}\dfrac{8\times10^4}{(s+5)(s+80)(s+0.1+j34)(s+0.1-j34)}1.1\times10^8 s}$$

and the steady-state error for a step external torque of magnitude, M_V, is

$$\frac{\theta_{Vss}}{M_V} = \left.\frac{1.05\times10^{-11}}{s^2+1.05\times10^{-11}\dfrac{1.45\times10^5}{(s+10)}\dfrac{30(s+1)}{(s+64)}\dfrac{8.8\times10^{12}}{(s+80)(s+0.1+j34)(s+0.1-j34)}}\right|_{s=0}$$

$$= 1.5\times10^{-12} \text{ radian/dyne-cm or } 3.1\times10^{-7} \text{ arc sec/dyne-cm}$$

To check this "stiffness" factor experimentally, a convenient source of external torque was provided by the gas jet normally used for unloading the controller. This jet reaction applied a known torque of 3.4×10^6 dyne-cm to the vehicle and a standoff angle of 1 arc second was measured. The calculated standoff angle is $(3.4\times10^6 \text{ dyne-cm})(3.1\times10^{-7} \text{ arc sec/dyne-cm}) = 1.05$ arc sec, which agrees well with the measured value.

CONCLUDING REMARKS

This investigation has shown that a twin-gyro attitude control system can stabilize a large space vehicle. The accuracy in attitude of the system used was maintained to better than 1 second of arc when external torques were less than 3×10^6 dyne-cm.

The system transfer function was derived analytically and the calculated frequency response was shown to agree closely with the measured frequency response.

One desirable feature of the twin-gyro controller is that it produces torque which is always directed about a single axis regardless of the gimbal angles. This feature allows the use of large gimbal angles so that a major portion of the momentum stored in the gyros is available for transfer to the vehicle. An advantage is therefore obtained over a single-gyro controller which must be restricted in gimbal angle to minimize cross-coupling torques.

Redundancy is inherent in the twin-gyro system in that it continues to function with loss of one gyro in any controller, although with correspondingly reduced performance.

Ideally, pairs of controller gyros may be turned on or off without inducing disturbance torques on the vehicle. Also, theoretically, with the particular orientation of controllers used in this investigation, selected sets of three gyros may be turned on or off, with no disturbance torques being developed. The ability to turn gyros on and off during a mission may be an important advantage if power conservation is a major factor.

In summary, the twin-gyro attitude control system would be especially adaptable to space vehicles which require precise attitude control with high dynamic response and low values of cross-coupling torque.

Ames Research Center
National Aeronautics and Space Administration
Moffett Field, Calif., April 20, 1964

APPENDIX A

NOTATION

$\bar{E}$	unit vector indicated by its index (i = 1, 2, or 3) which is a member of an orthogonal set fixed in the item indicated by a subscript
e	voltage within the control system
$\bar{H}$	vector angular momentum with respect to inertial space of item subscripted
$\dot{\bar{H}}$	vector derivative of $\bar{H}$ with respect to time
h	scalar magnitude of the angular momentum of the gyro element with respect to its spin axis
j	imaginary number, $\sqrt{-1}$
K	constant used for gains
$\bar{M}$	vector sum of external disturbance torques applied to the vehicle
m	torque applied to the subscripted item
s	Laplace operator
$\bar{W}$	vector angular velocity with respect to inertial space of the subscripted item
$\dot{\bar{W}}$	vector derivative of $\bar{W}$ with respect to time
x	vehicle roll axis having the direction $\bar{E}_{V1}$
y	vehicle pitch axis having the direction $\bar{E}_{V2}$
z	vehicle yaw axis having the direction $\bar{E}_{V3}$
Θ	constant gimbal offset angle
θ	angle through which the subscripted item has rotated with respect to a reference
$\dot{\theta}$	scalar derivative of θ with respect to time
$\bar{\bar{\Phi}}$	momental dyadic of the subscripted item
φ	scalar component (indicated by superscripts) of the momental dyadic of the subscripted item

τ	time constant
ω	scalar component of $\bar{W}$ along the vehicle coordinate direction indicated by the subscript
$\dot{\omega}$	time derivative of ω

Subscripts

b	vehicle minus the twin-gyro control system
c	twin-gyro controller
cx	x axis controller (roll)
cy	y axis controller (pitch)
cz	z axis controller (yaw)
f	frame of the twin-gyro controller
g	gimbal
ge	gyro element
ga	gimbal of gyro "a"
gb	gimbal of gyro "b"
i	index used as a subscript or a superscript
p	perturbation
r	reference set of directions fixed in the gyro case
ra	reference set of directions for gyro "a"
rb	reference set of directions for gyro "b"
s	attitude error sensor
ss	steady state
tsm	torque-summing member
v	vehicle

APPENDIX B

THE EQUATIONS OF MOTION OF AN IDEAL SINGLE-DEGREE-OF-FREEDOM GYRO

An "ideal" single-degree-of-freedom gyro will, for the purpose of this analysis, be specified as the one which meets the following definitions and requirements:

Definitions

1. The gimbal consists of a torque-summing member plus a gyro element (wheel).

2. The torque-summing member (tsm) consists of a support for the gyro element, a position pickoff device to measure the angle between the torque-summing member and the case, and a torque motor through which a torque may be applied between the torque-summing member and the case.

3. The gyro consists of a gimbal pivoted about one axis within a case.

Requirements

1. The components from which the gyro is assembled are rigid.

2. The gimbal must be free to rotate with respect to its case about an axis normal to the axis of rotation of the gyro element.

3. The center of mass of the gyro element is considered to remain located at the center of mass of the torque-summing member.

4. The mass distribution of the gimbal is considered to be symmetrical with respect to its three principal axes.

5. The gyro element is considered to rotate about its axis of symmetry at a constant angular velocity with respect to the torque-summing member.

6. The angle measured by the pickoff and the torque applied by the torque motor is considered to have zero error.

Let the unit vector $\bar{E}_{g1}$ be fixed in the gimbal and have the direction of the angular velocity of the gyro element with respect to the torque-summing member, as shown in the following sketch. Let the unit vector $\bar{E}_{g3}$

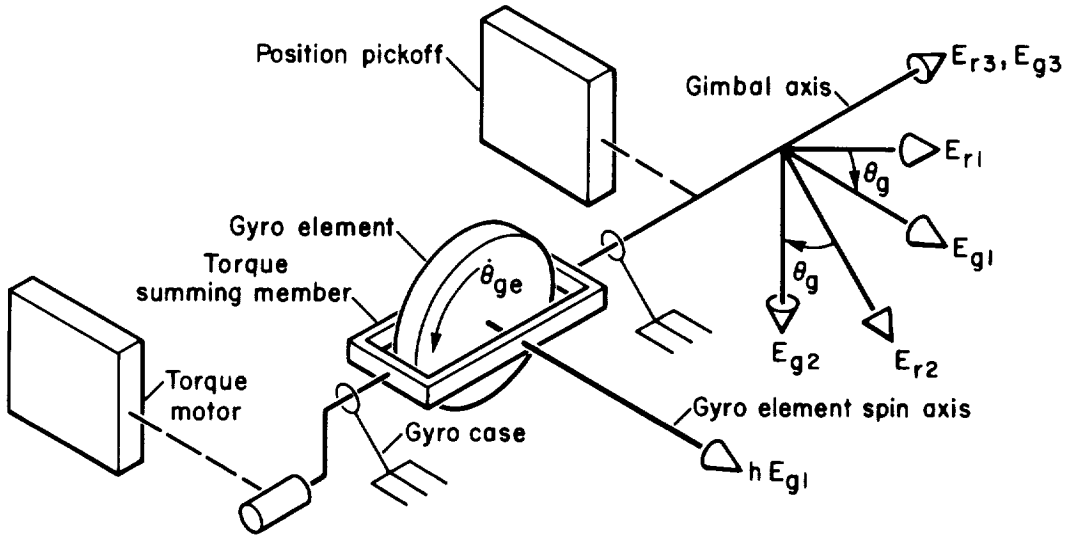

Coordinate systems for a single-degree-of-freedom gyro.

be fixed on the axis of rotation of the gimbal with respect to the case and have the direction from the center of mass of the gimbal toward the end of the gimbal containing the pickoff. Let the unit vector $\bar{E}_{g2}$ be defined by the relation

$$\bar{E}_{g2} = \bar{E}_{g3} \times \bar{E}_{g1} \tag{B1}$$

Let a second orthogonal set of unit vectors be chosen as reference vectors which are fixed in the case. Choose the orientation of these vectors such that when the output of the pickoff is zero, the two sets of vectors are related by

$$\bar{E}_{ri} = \bar{E}_{gi} \qquad (i = 1, 2, 3) \tag{B2}$$

where a repeated subscript not included within parentheses represents a summation subscript having the range 1, 2, and 3.

Let the angle of the gimbal with respect to the case be defined as positive when the gimbal rotates with its angular velocity with respect to the case in the direction of $\bar{E}_{g3}$.

Since momentum is a linear vector quantity, the angular momentum of the gimbal may be expressed as

$$\bar{H}_g = \bar{H}_{ge} + \bar{H}_{tsm} \tag{B3}$$

The angular momentum of a physical body may be expressed at the inner product of its momental dyadic with its angular velocity. Therefore, equation (B3) may be rewritten as

$$\bar{H}_g = \bar{\bar{\Phi}}_{ge} \cdot \bar{W}_{ge} + \bar{\bar{\Phi}}_{tsm} \cdot \bar{W}_{tsm} \tag{B4}$$

where $\bar{\bar{\Phi}}_{ge}$ and $\bar{\bar{\Phi}}_{tsm}$ are the momental dyadics of the gyro element and torque-summing member, respectively. Since $\bar{W}_{ge}$ is a linear vector quantity, it may be resolved into the two vectors

$$\bar{W}_{ge} = (\dot{\theta}_{ge})\bar{E}_{g1} + \bar{W}_{tsm} \tag{B5}$$

Therefore, equation (B4) may be written

$$\bar{H}_g = \dot{\theta}_{ge}\bar{\bar{\Phi}}_{ge} \cdot \bar{E}_{g1} + (\bar{\bar{\Phi}}_{ge} + \bar{\bar{\Phi}}_{tsm}) \cdot \bar{W}_g \tag{B6}$$

where

$$\bar{W}_{tsm} = \bar{W}_g$$

The principal directions of $\bar{\bar{\Phi}}_{ge}$ are equal to the gimbal coordinate directions $\bar{E}_{gi}$ (i = 1, 2, 3) because the direction of the axis of symmetry of the gyro element is the same as $\bar{E}_{g1}$. Therefore, the momental dyadic of the gyro element may be expressed as

$$\bar{\bar{\Phi}}_{ge} = \varphi_{ge}^{ii}\bar{E}_{gi}\bar{E}_{gi} \qquad \text{(summed on i)} \tag{B7}$$

where the products of inertia have vanished because of the required symmetry.

Since the unit vectors $\bar{E}_{gi}$ (i = 1, 2, 3) are fixed with respect to the torque-summing member and are its principal directions, then the momental dyadic of the torque-summing member may be written as

$$\bar{\bar{\Phi}}_{tsm} = \varphi_{tsm}^{ii}\bar{E}_{gi}\bar{E}_{gi} \tag{B8}$$

Since the momental dyadics of both the gyro element and the torque-summing member are linear dyadics referred to the same set of directions they may be summed directly to obtain

$$\bar{\bar{\Phi}}_g = \bar{\bar{\Phi}}_{ge} + \bar{\bar{\Phi}}_{tsm} \tag{B9}$$

where the components are

$$\varphi_g^{ii} = \varphi_{ge}^{ii} + \varphi_{tsm}^{ii} \qquad (i = 1, 2, 3) \tag{B10}$$

Also, because it was required that the mass distribution of the gimbal be symmetrical about $\bar{E}_{g3}$ and since $\bar{E}_{g3} = \bar{E}_{r3}$ then the momental dyadic of the gimbal may be expressed in terms of the reference coordinate system by means of

$$\bar{\bar{\Phi}}_g = \varphi_g^{ii}\bar{E}_{ri}\bar{E}_{ri} \tag{B11}$$

At this point, equation (B6) may be written

$$\bar{H}_g = h\bar{E}_{g1} + \bar{\bar{\Phi}}_g \cdot \bar{W}_g \tag{B12}$$

where

$$h = \dot{\theta}_{ge}\varphi_{ge}^{11} = \text{constant}$$

Since $\bar{W}_g$ is a linear vector quantity, it may be expressed as

$$\bar{W}_g = \dot{\theta}_g\bar{E}_{g3} + \bar{W}_r = \dot{\theta}_g\bar{E}_{r3} + \bar{W}_r \tag{B13}$$

also $\bar{E}_{g1}$ may be expressed in terms of the reference unit vectors by means of the idemfactor (unit dyadic) as

$$\begin{aligned} \bar{E}_{g1} &= \bar{E}_{g1} \cdot \bar{E}_{ri}\bar{E}_{ri} \qquad \text{(summed on } i\text{)} \\ &= \cos\theta_g\bar{E}_{r1} + \sin\theta_g\bar{E}_{r2} \end{aligned} \tag{B14}$$

Therefore, the momentum of the gimbal may be expressed as

$$\bar{H}_g = h\cos\theta_g\bar{E}_{r1} + h\sin\theta_g\bar{E}_{r2} + \dot{\theta}_g\varphi_g^{33}\bar{E}_{r3} + \bar{\bar{\Phi}}_g \cdot \bar{W}_r \tag{B15}$$

If the total derivative of equation (B15) is taken with respect to time, the time rate of change of momentum of the gimbal is

$$\begin{aligned} \dot{\bar{H}}_g = {} & -h\dot{\theta}_g\sin\theta_g\bar{E}_{r1} + h\dot{\theta}_g\cos\theta_g\bar{E}_{r2} + \varphi_g^{33}\ddot{\theta}_g\bar{E}_{r3} + W_r \times h\cos\theta_g\bar{E}_{r1} \\ & + \bar{W}_r \times \left(h\sin\theta_g\bar{E}_{r2} + \varphi_g^{33}\dot{\theta}_g\bar{E}_{r3}\right) + \dot{\bar{\bar{\Phi}}}_g \cdot \bar{W}_r + \bar{W}_r \times \bar{\bar{\Phi}}_g \cdot \bar{W}_r \end{aligned} \tag{B16}$$

The vector $\bar{W}_r$ may be expressed in terms of the idemfactor (unit dyadic) of the orthogonal reference coordinate system by means of

$$\bar{W}_r = \bar{W}_r \cdot \bar{E}_{ri}\bar{E}_{ri} \qquad \text{(summed on i)} \tag{B17}$$

If equation (B17) is substituted into equation (B16), the operations are performed as indicated, and the terms are collected, then the time rate of change of the momentum of the gimbal may be expressed as

$$\begin{aligned}\dot{\bar{H}}_g = {} & \left[-h\dot{\theta}_g \sin\theta_g + \varphi_g^{33}\dot{\theta}_g\left(\bar{W}_r \cdot \bar{E}_{r2}\right) - h \sin\theta_g\left(\bar{W}_r \cdot \bar{E}_{r3}\right)\right]\bar{E}_{r1} + \left[h\dot{\theta}_g \cos\theta_g\right. \\ & \left. + h \cos\theta_g\left(\bar{W}_r \cdot \bar{E}_{r3}\right) - \varphi_g^{33}\dot{\theta}_g\left(\bar{W}_r \cdot \bar{E}_{r1}\right)\right]\bar{E}_{r2} \\ & + \left[\varphi_g^{33}\ddot{\theta}_g + h \sin\theta_g\left(\bar{W}_r \cdot \bar{E}_{r1}\right) - h \cos\theta_g\left(\bar{W}_r \cdot \bar{E}_{r2}\right)\right]\bar{E}_{r3} + \bar{\bar{\Phi}}_g \cdot \dot{\bar{W}}_r \\ & + \bar{W}_r \times \bar{\bar{\Phi}}_g \cdot \bar{W}_r\end{aligned} \tag{B18}$$

Let m_g be defined as the magnitude of the torque applied to the gimbal by the torque motor.

Then $m_g = \dot{\bar{H}}_g \cdot \bar{E}_{r3}$ and since $\varphi_g^{11} = \varphi_g^{22}$

$$m_g = \varphi_g^{33}\left[\left(\dot{\bar{W}}_r \cdot \bar{E}_{r3}\right) + \ddot{\theta}_g\right] + h\left(\bar{W}_r \cdot \bar{E}_{r1}\right)\sin\theta_g - h\left(\bar{W}_r \cdot \bar{E}_{r2}\right)\cos\theta_g \tag{B19}$$

APPENDIX C

THE EQUATIONS OF MOTION OF AN IDEAL SINGLE-AXIS TWIN-GYRO CONTROLLER

For the purpose of this analysis, an ideal single-axis twin-gyro controller is defined as a twin-gyro controller which meets the following requirements (see fig. 2):

1. The controller is considered to consist of a rigid frame within which is mounted the gimbals of two identical, ideal gyros, and upon which is mounted the fixed portions of the torquers and pickoffs associated with the gimbals.

2. An orthogonal right-hand set of unit vectors $\bar{E}_{ci}$ (i = 1, 2, 3) is considered to be fixed in the frame of the controller.

3. The ideal gimbal "a" and its associated components are oriented within the frame of the controller so that the gimbal's reference unit vectors $\bar{E}_{rai}$ (i = 1, 2, 3) may be transformed to the controller unit vectors by means of

$$\bar{E}_{ra1} = \bar{E}_{c1} , \qquad \bar{E}_{ra2} = \bar{E}_{c2} , \qquad \bar{E}_{ra3} = \bar{E}_{c3}$$

4. The ideal gimbal "b" and its associated components are oriented within the frame of the controller so that the gimbal's reference unit vectors $\bar{E}_{rbi}$ (i = 1, 2, 3) may be transformed to the controller unit vectors by means of

$$\bar{E}_{rb1} = -\bar{E}_{c1} , \qquad \bar{E}_{rb2} = -\bar{E}_{c2} , \qquad \bar{E}_{rb3} = \bar{E}_{c3}$$

5. Whenever gimbal "a" rotates with respect to the frame through an angle $\theta_{ga} = \theta_c$, then gimbal "b" is required to be forced by its torquer to rotate with respect to the frame through the angle $\theta_{gb} = -\theta_c$.

The angular momentum of the controller in inertial space may be expressed as the sum of the angular momenta in inertial space of the individual components of the controller:

$$\begin{aligned} \bar{H}_c &= \bar{H}_{ga} + \bar{H}_{gb} + \bar{H}_f \\ &= \bar{H}_{ga} + \bar{H}_{gb} + \bar{\bar{\Phi}}_f \cdot \bar{W}_c \end{aligned} \tag{C1}$$

where $\bar{\bar{\Phi}}_f$ is the momental dyadic of the fixed portions of the controller and W_c is the angular velocity of the controller with respect to inertial space.

The time rate of change of angular momentum of the controller may then be written

$$\dot{\bar{H}}_c = \dot{\bar{H}}_{ga} + \dot{\bar{H}}_{gb} + \bar{\bar{\Phi}}_f \cdot \dot{\bar{W}}_c + \bar{W}_c \times \bar{\bar{\Phi}}_f \cdot \bar{W}_c \tag{C2}$$

From appendix B, $\dot{\bar{H}}_{ga}$ may be written

$$\begin{aligned}\dot{\bar{H}}_{ga} = {} & \left[-h\dot{\theta}_{ga} \sin \theta_{ga} + \varphi_g^{33}\dot{\theta}_{ga}\left(\bar{W}_c \cdot \bar{E}_{ra2}\right) - h \sin \theta_{ga}\left(\bar{W}_c \cdot \bar{E}_{ra3}\right)\right] \bar{E}_{ra1} \\ & + \left[h\dot{\theta}_{ga} \cos \theta_{ga} + h \cos \theta_{ga}\left(\bar{W}_c \cdot \bar{E}_{ra3}\right) - \varphi_g^{33}\dot{\theta}_{ga}\left(\bar{W}_c \cdot \bar{E}_{ra1}\right)\right] \bar{E}_{ra2} \\ & + \left[\varphi_g^{33}\ddot{\theta}_{ga} + h \sin \theta_{ga}\left(\bar{W}_c \cdot \bar{E}_{ra1}\right) - h \cos \theta_{ga}\left(\bar{W}_c \cdot \bar{E}_{ra2}\right)\right] \bar{E}_{ra3} \\ & + \bar{\bar{\Phi}}_{ga} \cdot \dot{\bar{W}}_c + \bar{W}_c \times \bar{\bar{\Phi}}_{ga} \cdot \bar{W}_c \end{aligned} \tag{C3}$$

Similarly, from appendix B, $\dot{\bar{H}}_{gb}$ may be written

$$\begin{aligned}\dot{\bar{H}}_{gb} = {} & \left[-h\dot{\theta}_{gb} \sin \theta_{gb} + \varphi_g^{33}\dot{\theta}_{gb}\left(\bar{W}_c \cdot \bar{E}_{rb2}\right) - h \sin \theta_{gb}\left(\bar{W}_c \cdot \bar{E}_{rb3}\right)\right] \bar{E}_{rb1} \\ & + \left[h\dot{\theta}_{gb} \cos \theta_{gb} + h \cos \theta_{gb}\left(\bar{W}_c \cdot \bar{E}_{rb3}\right) - \varphi_g^{33}\dot{\theta}_{gb}\left(\bar{W}_c \cdot \bar{E}_{rb1}\right)\right] \bar{E}_{rb2} \\ & + \left[\varphi_g^{33}\ddot{\theta}_{gb} + h \sin \theta_{gb}\left(\bar{W}_c \cdot \bar{E}_{rb1}\right) - h \cos \theta_{gb}\left(\bar{W}_c \cdot \bar{E}_{rb2}\right)\right] \bar{E}_{rb3} \\ & + \bar{\bar{\Phi}}_{gb} \cdot \dot{\bar{W}}_c + \bar{W}_c \times \bar{\bar{\Phi}}_{gb} \cdot \bar{W}_c \end{aligned} \tag{C4}$$

Since the gimbals have symmetrical mass distribution their momental dyadics may be expressed in terms of the controller unit vectors. Therefore

$$\bar{\bar{\Phi}}_c = \bar{\bar{\Phi}}_{ga} + \bar{\bar{\Phi}}_{gb} + \bar{\bar{\Phi}}_f \tag{C5}$$

where

$$\bar{\bar{\Phi}}_c = \varphi_c^{ii}\bar{E}_{ci}\bar{E}_{ci} \qquad \text{(summed on i)}$$

Then if the unit vectors of gimbals "a" and "b" are transformed according to the controller requirements 3 and 4 and substituted into equation (C2), one may write

$$\dot{\bar{H}}_c = \left[-h\left(\dot{\theta}_{ga} \sin\theta_{ga} - \dot{\theta}_{gb} \sin\theta_{gb}\right) + \varphi_g^{33}\left(\dot{\theta}_{ga} + \dot{\theta}_{gb}\right)\left(\bar{W}_c \cdot \bar{E}_{c2}\right) \right.$$

$$\left. - h\left(\sin\theta_{ga} - \sin\theta_{gb}\right)\left(\bar{W}_c \cdot \bar{E}_{c3}\right)\right] \bar{E}_{c1} + \left[h\left(\dot{\theta}_{ga} \cos\theta_{ga} - \dot{\theta}_{gb} \cos\theta_{gb}\right)\right.$$

$$\left. - \varphi_g^{33}\left(\dot{\theta}_{ga} + \dot{\theta}_{gb}\right)\left(\bar{W}_c \cdot \bar{E}_{c1}\right) + h\left(\cos\theta_{ga} - \cos\theta_{gb}\right)\left(\bar{W}_c \cdot \bar{E}_{c3}\right)\right] \bar{E}_{c2}$$

$$+ \left[\varphi_g^{33}\left(\ddot{\theta}_{ga} + \ddot{\theta}_{gb}\right) + h\left(\sin\theta_{ga} - \sin\theta_{gb}\right)\left(\bar{W}_c \cdot \bar{E}_{c1}\right)\right.$$

$$\left. - h\left(\cos\theta_{ga} - \cos\theta_{gb}\right)\left(\bar{W}_c \cdot \bar{E}_{c2}\right)\right] \bar{E}_{c3} + \bar{\bar{\Phi}}_c \cdot \dot{\bar{W}}_c + \bar{W}_c \times \bar{\bar{\Phi}}_c \cdot \bar{W}_c \qquad (C6)$$

If the requirement that $\theta_{ga} = \theta_c$ and $\theta_{gb} = -\theta_c$ is now imposed, the time rate of change of momentum of the controller may be expressed as

$$\dot{\bar{H}}_c = -2h \sin\theta_c \left(\bar{W}_c \cdot \bar{E}_{c3}\right) \bar{E}_{c1} + 2h\dot{\theta}_c \cos\theta_c \bar{E}_{c2}$$

$$+ 2h \sin\theta_c \left(\bar{W}_c \cdot \bar{E}_{c1}\right) \bar{E}_{c3} + \bar{\bar{\Phi}}_c \cdot \dot{\bar{W}}_c + \bar{W}_c \times \bar{\bar{\Phi}}_c \cdot \bar{W}_c \qquad (C7)$$

Let m_{ga} and m_{gb} be defined as the magnitude of the torques applied to gimbal "a" and gimbal "b" by their respective torquer motors. In terms of $\dot{W}_c$ and W_c, these values from equation (B19) may be expressed as

$$m_{ga} = \varphi_g^{33}\left[\left(\dot{\bar{W}}_c \cdot \bar{E}_{ra3}\right) + \ddot{\theta}_{ga}\right] + h\left[\left(\bar{W}_c \cdot \bar{E}_{ra1}\right) \sin\theta_{ga} - \left(\bar{W}_c \cdot \bar{E}_{ra2}\right) \cos\theta_{ga}\right] \qquad (C8)$$

$$m_{gb} = \varphi_g^{33}\left[\left(\dot{\bar{W}}_c \cdot \bar{E}_{rb3}\right) + \ddot{\theta}_{gb}\right] + h\left[\left(\bar{W}_c \cdot \bar{E}_{rb1}\right) \sin\theta_{gb} - \left(\bar{W}_c \cdot \bar{E}_{rb2}\right) \cos\theta_{gb}\right] \qquad (C9)$$

If these equations are transformed into controller coordinates and the controller parameter θ_c then

$$m_{ga} = \varphi_g^{33}\left[\left(\dot{\bar{W}}_c \cdot \bar{E}_{c3}\right) + \ddot{\theta}_c\right] + h\left[\left(\bar{W}_c \cdot \bar{E}_{c1}\right) \sin\theta_c - \left(\bar{W}_c \cdot \bar{E}_{c2}\right) \cos\theta_c\right] \qquad (C10)$$

$$m_{gb} = \varphi_g^{33}\left[\left(\dot{\overline{W}}_c \cdot \overline{E}_{c3}\right) - \ddot{\theta}_c\right] + h\left[\left(\overline{W}_c \cdot \overline{E}_{c1}\right)\sin\theta_c + \left(\overline{W}_c \cdot \overline{E}_{c2}\right)\cos\theta_c\right] \tag{C11}$$

Since the gyros are slaved to move in equal and opposite directions,

$$m_{ga} = -m_{gb} \tag{C12}$$

Substituting equation (C12) into (C11), changing sign, and adding to (C10) results in

$$m_g = \varphi_g^{33}\ddot{\theta}_c - h\left(\overline{W}_c \cdot \overline{E}_{c2}\right)\cos\theta_c \tag{C13}$$

which is the equation of motion of an ideal, single-axis, twin-gyro controller.

APPENDIX D

THE EQUATIONS OF MOTION OF A THREE-AXIS TWIN-GYRO ATTITUDE CONTROL SYSTEM

To describe the behavior of a space vehicle with a twin-gyro attitude control system on board, an ideal condition is considered. The gyro equations are simplified by specifying a symmetrical mass distribution in the gyro gimbals as defined in appendix B. It is further assumed that the vehicle is a rigid body, and that its principal axes of inertia coincide with the vehicle axes x, y, and z which are defined in the directions of three unit vectors $\overline{E}_{vi}$ (i = 1, 2, 3), respectively. Three identical single-axis twin-gyro controllers are assumed to be rigidly mounted on the vehicle. These controllers are considered to be ideal, as described in appendix C.

The three single-axis twin-gyro controllers are assumed to be oriented with respect to the space vehicle so that each axis of the vehicle has one controller associated with it. Therefore, they are identified as the x axis controller, the y axis controller, and the z axis controller. Also, they are assumed to be oriented with respect to the vehicle as described by the following relations between the controller reference vectors, $\overline{E}_{ci}$, and the vehicle reference vectors, $\overline{E}_{vi}$ (i = 1, 2, 3) (see fig. 7).

For the x axis controller,

$$\overline{E}_{cx1} = \frac{\sqrt{2}}{2}\left(\overline{E}_{v3} - \overline{E}_{v2}\right)$$

$$\overline{E}_{cx2} = \overline{E}_{v1}$$

$$\overline{E}_{cx3} = \frac{\sqrt{2}}{2}\left(\overline{E}_{v3} + \overline{E}_{v2}\right)$$

For the y axis controller,

$$\overline{E}_{cy1} = \frac{\sqrt{2}}{2}\left(\overline{E}_{v1} - \overline{E}_{v3}\right)$$

$$\overline{E}_{cy2} = \overline{E}_{v2}$$

$$\overline{E}_{cy3} = \frac{\sqrt{2}}{2}\left(\overline{E}_{v1} + \overline{E}_{v3}\right)$$

For the z axis controller,

$$\bar{E}_{cz1} = \frac{\sqrt{2}}{2}\left(\bar{E}_{v2} - \bar{E}_{v1}\right)$$

$$\bar{E}_{cz2} = \bar{E}_{v3}$$

$$\bar{E}_{cz3} = \frac{\sqrt{2}}{2}\left(\bar{E}_{v2} + \bar{E}_{v1}\right)$$

While this orientation is not required for a twin-gyro attitude control system, it is the one used in the experimental research associated with this report.

The time rate of change of the angular momentum of an ideal single-axis twin-gyro controller as derived in appendix C is expressed in terms of the controller-fixed set of reference vectors $\bar{E}_{ci}$:

$$\dot{\bar{H}}_c = -2h\left(\bar{W}_c \cdot \bar{E}_{c3}\right)\sin\theta_c\bar{E}_{c1} + 2h\dot{\theta}_c\cos\theta_c\bar{E}_{c2} + 2h\left(\bar{W}_c \cdot \bar{E}_{c1}\right)\sin\theta_c\bar{E}_{c3}$$
$$+ \bar{\bar{\Phi}}_c \cdot \dot{\bar{W}}_c + \bar{W}_c \times \bar{\bar{\Phi}}_c \cdot \bar{W}_c \qquad (D1)$$

Since the single-axis twin-gyro controllers have been assumed to be rigidly attached to the space vehicle, the angular velocity of the controller with respect to inertial space is identical to the angular velocity of the vehicle with respect to inertial space. Therefore, the terms $\bar{W}_c$ and $\dot{\bar{W}}_c$ in equation (D1) may be replaced with $\bar{W}_v$ and $\dot{\bar{W}}_v$, respectively, which becomes

$$\dot{\bar{H}}_c = -2h\left(\bar{W}_v \cdot \bar{E}_{c3}\right)\sin\theta_c\bar{E}_{c1} + 2h\dot{\theta}_c\cos\theta_c\bar{E}_{c2} + 2h\left(\bar{W}_v \cdot \bar{E}_{c1}\right)\sin\theta_c\bar{E}_{c3}$$
$$+ \bar{\bar{\Phi}}_c \cdot \dot{\bar{W}}_v + \bar{W}_v \times \bar{\bar{\Phi}}_c \cdot \bar{W}_v \qquad (D2)$$

If the controller set of unit vectors is transformed into the vehicle set of unit vectors, then for the x axis controller,

$$\dot{\bar{H}}_{cx} = 2h\left(\bar{W}_v \cdot \bar{E}_{v3}\right)\sin\theta_{cx}\bar{E}_{v2} + 2h\dot{\theta}_{cx}\cos\theta_{cx}\,\bar{E}_{v1} - 2h\left(\bar{W}_v \cdot \bar{E}_{v2}\right)\sin\theta_{cx}\bar{E}_{v3}$$
$$+ \bar{\bar{\Phi}}_{cx} \cdot \dot{\bar{W}}_v + \bar{W}_v \times \bar{\bar{\Phi}}_{cx} \cdot \bar{W}_v \qquad (D3)$$

for the y axis controller,

$$\dot{\bar{H}}_{cy} = -2h\left(\bar{W}_v \cdot \bar{E}_{v3}\right)\sin\theta_{cy}\bar{E}_{v1} + 2h\dot{\theta}_{cy}\cos\theta_{cy}\bar{E}_{v2} + 2h\left(\bar{W}_v \cdot \bar{E}_{v1}\right)\sin\theta_{cy}\bar{E}_{v3}$$
$$+ \bar{\bar{\Phi}}_{cy} \cdot \dot{\bar{W}}_v + \bar{W}_v \times \bar{\bar{\Phi}}_{cy} \cdot \bar{W}_v \qquad (D4)$$

and for the z axis controller,

$$\dot{\bar{H}}_{cz} = 2h\left(\bar{W}_v \cdot \bar{E}_{v2}\right) \sin \theta_{cz}\bar{E}_{v1} + 2h\dot{\theta}_{cz} \cos \theta_{cz}\bar{E}_{v3} - 2h\left(\bar{W}_v \cdot \bar{E}_{v1}\right) \sin \theta_{cz}\bar{E}_{v2}$$
$$+ \bar{\bar{\Phi}}_{cz} \cdot \dot{\bar{W}}_v + \bar{W}_v \times \bar{\bar{\Phi}}_{cz} \cdot \bar{W}_v \qquad \text{(D5)}$$

If $\bar{\bar{\Phi}}_v$ is defined as the momental dyadic of the entire vehicle, including the controllers, then $\bar{\bar{\Phi}}_b$ may be defined as the momental dyadic of the vehicle, less the three controllers, and

$$\bar{\bar{\Phi}}_b = \bar{\bar{\Phi}}_v - \bar{\bar{\Phi}}_{cx} - \bar{\bar{\Phi}}_{cy} - \bar{\bar{\Phi}}_{cz} \qquad \text{(D6)}$$

Then the angular momentum of the vehicle, less the three controllers, may be expressed as

$$\bar{H}_b = \bar{\bar{\Phi}}_b \cdot \bar{W}_v \qquad \text{(D7)}$$

The time rate of change of the angular momentum of the vehicle without the controllers may then be written

$$\dot{\bar{H}}_b = \bar{\bar{\Phi}}_b \cdot \dot{\bar{W}}_v + \bar{W}_v \times \bar{\bar{\Phi}}_b \cdot \bar{W}_v \qquad \text{(D8)}$$

The time rate of change of angular momentum of the entire vehicle, $\dot{\bar{H}}_v$, is equal to the vector sum of the time rate of change of angular momentum of each of its parts. Therefore,

$$\dot{\bar{H}}_v = \dot{\bar{H}}_b + \dot{\bar{H}}_{cx} + \dot{\bar{H}}_{cy} + \dot{\bar{H}}_{cz} \qquad \text{(D9)}$$

and when equations (D3), (D4), (D5), and (D8) are substituted into equation (D9), the time rate of change of angular momentum of the entire vehicle may be written as

$$\dot{\bar{H}}_v = \bar{\bar{\Phi}}_v \cdot \dot{\bar{W}}_v + \bar{W}_v \times \bar{\bar{\Phi}}_v \cdot \bar{W}_v + 2h\left[\dot{\theta}_{cx} \cos \theta_{cx} - \left(\bar{W}_v \cdot \bar{E}_{v3}\right) \sin \theta_{cy}\right.$$
$$\left. + \left(\bar{W}_v \cdot \bar{E}_{v2}\right) \sin \theta_{cz}\right] \bar{E}_{v1} + 2h\left[\dot{\theta}_{cy} \cos \theta_{cy} - \left(\bar{W}_v \cdot \bar{E}_{v1}\right) \sin \theta_{cz}\right.$$
$$\left. + \left(\bar{W}_v \cdot \bar{E}_{v3}\right) \sin \theta_{cx}\right] \bar{E}_{v2} + 2h\left[\dot{\theta}_{cz} \cos \theta_{cz} - \left(\bar{W}_v \cdot \bar{E}_{v2}\right) \sin \theta_{cx}\right.$$
$$\left. + \left(\bar{W}_v \cdot \bar{E}_{v1}\right) \sin \theta_{cy}\right] \bar{E}_{v3} \qquad \text{(D10)}$$

The vector angular velocity and angular acceleration of the vehicle with respect to inertial space may be resolved along the vehicle axes by means of the relations

$$\bar{W}_V = \omega_1 \bar{E}_{V1} + \omega_2 \bar{E}_{V2} + \omega_3 \bar{E}_{V3} \tag{D11}$$

$$\dot{\bar{W}}_V = \dot{\omega}_1 \bar{E}_{V1} + \dot{\omega}_2 \bar{E}_{V2} + \dot{\omega}_3 \bar{E}_{V3} \tag{D12}$$

Also, since the vehicle axes were chosen to lie along the vehicle axes of symmetry, the momental dyadic of the vehicle may be expressed as

$$\bar{\bar{\Phi}}_V = \varphi_V^{11} \bar{E}_{V1} \bar{E}_{V1} + \varphi_V^{22} \bar{E}_{V2} \bar{E}_{V2} + \varphi_V^{33} \bar{E}_{V3} \bar{E}_{V3} \tag{D13}$$

where $\varphi_V^{ii} \equiv$ the moment of inertia of the vehicle about the $\bar{E}_{Vi}$ axis ($i = 1, 2, 3$). When the above relations are substituted into equation (D10), the expression for the time rate of change of angular momentum of the vehicle becomes

$$\begin{aligned}
\dot{\bar{H}}_V = {} & \left[\varphi_V^{11} \dot{\omega}_1 + \left(\varphi_V^{33} - \varphi_V^{22} \right) \omega_2 \omega_3 \right] \bar{E}_{V1} \\
& + \left[\varphi_V^{22} \dot{\omega}_2 + \left(\varphi_V^{11} - \varphi_V^{33} \right) \omega_1 \omega_3 \right] \bar{E}_{V2} \\
& + \left[\varphi_V^{33} \dot{\omega}_3 + \left(\varphi_V^{22} - \varphi_V^{11} \right) \omega_1 \omega_2 \right] \bar{E}_{V3} \\
& + 2h \left(\dot{\theta}_{cx} \cos \theta_{cx} - \omega_3 \sin \theta_{cy} + \omega_2 \sin \theta_{cz} \right) \bar{E}_{V1} \\
& + 2h \left(\dot{\theta}_{cy} \cos \theta_{cy} - \omega_1 \sin \theta_{cz} + \omega_3 \sin \theta_{cx} \right) \bar{E}_{V2} \\
& + 2h \left(\dot{\theta}_{cz} \cos \theta_{cz} - \omega_2 \sin \theta_{cx} + \omega_1 \sin \theta_{cy} \right) \bar{E}_{V3}
\end{aligned} \tag{D14}$$

Equating the time rate of change of angular momentum to the sum of external moments results in the three equations of motion for the vehicle

$$\left.\begin{aligned}
\bar{M}_{Vx} &= \varphi_V^{11} \dot{\omega}_1 + \left(\varphi_V^{33} - \varphi_V^{22} \right) \omega_2 \omega_3 + 2h \left(\dot{\theta}_{cx} \cos \theta_{cx} - \omega_3 \sin \theta_{cy} + \omega_2 \sin \theta_{cz} \right) \\
\bar{M}_{Vy} &= \varphi_V^{22} \dot{\omega}_2 + \left(\varphi_V^{11} - \varphi_V^{33} \right) \omega_1 \omega_3 + 2h \left(\dot{\theta}_{cy} \cos \theta_{cy} - \omega_1 \sin \theta_{cz} + \omega_3 \sin \theta_{cx} \right) \\
\bar{M}_{Vz} &= \varphi_V^{33} \dot{\omega}_3 + \left(\varphi_V^{22} - \varphi_V^{11} \right) \omega_2 \omega_1 + 2h \left(\dot{\theta}_{cz} \cos \theta_{cz} - \omega_2 \sin \theta_{cx} + \omega_1 \sin \theta_{cy} \right)
\end{aligned}\right\} \tag{D15}$$

In addition to the above set of equations for the vehicle, there are equations for each of the twin-gyro controllers. From equation (C13), and using equation (D11)

$$\left.\begin{aligned} m_{gx} &= \varphi_g^{33}\ddot{\theta}_{cx} - h\omega_1 \cos \theta_{cx} \\ m_{gy} &= \varphi_g^{33}\ddot{\theta}_{cy} - h\omega_2 \cos \theta_{cy} \\ m_{gz} &= \varphi_g^{33}\ddot{\theta}_{cz} - h\omega_3 \cos \theta_{cz} \end{aligned}\right\} \tag{D16}$$

It should be noted that the controller subscripts indicate the vehicle axes controlled and not the locations of the controllers.

The gimbal torques used in the mechanized control system were of the following form:

$$\left.\begin{aligned} m_{gx} &= K_{1x}\theta_{v1} + K_{2x}\int \theta_{v1}\, dt - K_{3x}\dot{\theta}_{cx} - K_{4x}\theta_{cx} \\ m_{gy} &= K_{1y}\theta_{v2} + K_{2y}\int \theta_{v2}\, dt - K_{3y}\dot{\theta}_{cy} - K_{4y}\theta_{cy} \\ m_{gz} &= K_{1z}\theta_{v3} + K_{2z}\int \theta_{v3}\, dt - K_{3z}\dot{\theta}_{cz} - K_{4z}\theta_{cz} \end{aligned}\right\} \tag{D17}$$

Equations (D15), (D16), and (D17) are the complete equations of motion for the system.

In order to compare the equations of motion with the mechanized system, the following assumptions and simplifications are made:

1. The vehicle angular rates, ω_i, are expressed in terms of Euler angles, θ_{vi}, and those terms containing products of variables are neglected.

2. The gyro gimbal angles, θ_{ci}, are the sum of a constant angle, Θ_{ci}, and a perturbation, θ_{cip}, and the following small-angle approximations are used:

$$\sin \theta_{ci} = \sin\left(\Theta_{ci} + \theta_{cip}\right) \approx \sin \Theta_{ci} + \theta_{cip} \cos \Theta_{ci}$$

$$\cos \theta_{ci} = \cos\left(\Theta_{ci} + \theta_{cip}\right) \approx \cos \Theta_{ci} - \theta_{cip} \sin \Theta_{ci}$$

3. As a result of past history of motion of both the vehicle and the gyros, the gimbals will be offset to some angle, Θ_{ci}, and the integration feedback will have some initial condition value. It is

assumed that the system is in equilibrium to begin with, and that the signal from the gimbal position, Θ, exactly cancels the integrator initial condition signal.

With the above approximations, equations (D15), (D16), and (D17) become linear. The Laplace transforms of these equations take the following form, where the first three are vehicle equations and the remaining three are controller equations:

$$\left.\begin{aligned}
M_{vx}(s) &= \left(\varphi_v^{11}s^2\right)\theta_{v1}(s) + \left(2hs\,\sin\Theta_{cz}\right)\theta_{v2}(s) \\
&\quad - \left(2hs\,\sin\Theta_{cy}\right)\theta_{v3}(s) + \left(2hs\,\cos\Theta_{cx}\right)\theta_{cxp}(s) \\
M_{vy}(s) &= -\left(2hs\,\sin\Theta_{cz}\right)\theta_{v1}(s) + \left(\varphi_v^{22}s^2\right)\theta_{v2}(s) \\
&\quad + \left(2hs\,\sin\Theta_{cx}\right)\theta_{v3}(s) + \left(2hs\,\cos\Theta_{cy}\right)\theta_{cyp}(s) \\
M_{vz}(s) &= \left(2hs\,\sin\Theta_{cy}\right)\theta_{v1}(s) - \left(2hs\,\sin\Theta_{cx}\right)\theta_{v2}(s) \\
&\quad + \left(\varphi_v^{33}s^2\right)\theta_{v3}(s) + \left(2hs\,\cos\Theta_{cz}\right)\theta_{czp}(s)
\end{aligned}\right\} \qquad (D18)$$

$$\left.\begin{aligned}
\left(\varphi_g^{33}s^2 + K_{3x}s + K_{4x}\right)\theta_{cxp}(s) - \left(K_{1x} + K_{2x}/s + hs\,\cos\Theta_{cx}\right)\theta_{v1}(s) &= 0 \\
\left(\varphi_g^{33}s^2 + K_{3y}s + K_{4y}\right)\theta_{cyp}(s) - \left(K_{1y} + K_{2y}/s + hs\,\cos\Theta_{cy}\right)\theta_{v2}(s) &= 0 \\
\left(\varphi_g^{33}s^2 + K_{3z}s + K_{4z}\right)\theta_{czp}(s) - \left(K_{1z} + K_{2z}/s + hs\,\cos\Theta_{cz}\right)\theta_{v3}(s) &= 0
\end{aligned}\right\} \qquad (D19)$$

In order to compare the above equations with the mechanized system it is desirable to look at the equations for a single axis. This may be accomplished, and the equations decoupled, by assuming that the gyro gimbal angles are zero for at least two axes. If the roll and pitch gyro gimbals are at zero angle, the following yaw axis equations result:

$$\left(\varphi_v^{33}s^2\right)\theta_{v3}(s) + \left(2hs\,\cos\Theta_{cz}\right)\theta_{czp}(s) = M_{vz}(s) \qquad (D20)$$

$$\left(\varphi_g^{33}s^2 + K_{3z}s + K_{4z}\right)\theta_{czp}(s) - \left(K_{1z} + K_{2z}/s + hs\,\cos\Theta_{cz}\right)\theta_{v3}(s) = 0 \qquad (D21)$$

These equations yield the single-axis transfer function for vehicle response to external torque input

$$\frac{\theta_{V3}(s)}{M_{V3}(s)} = \frac{\varphi_g^{33}s^2 + K_{3Z}s + K_{4Z}}{\left(\varphi_V^{33}s^2\right)\left(\varphi_g^{33}s^2 + K_{3Z}s + K_{4Z}\right) + 2hs\cos\Theta_{CZ}\left(K_{1Z} + K_{2Z}/s + hs\cos\Theta_{CZ}\right)} \tag{D22}$$

REFERENCES

1. White, John S., and Hansen, Q. Marion: Study of Systems Using Inertia Wheels for Precise Attitude Control of a Satellite. NASA TN D-691, 1961.

2. White, John S., Shigemoto, Fred H., and Bourquin, Kent: Satellite Attitude Control Utilizing the Earth's Magnetic Field. NASA TN D-1068, 1961.

3. White, John S., and Hansen, Q. Marion: Study of a Satellite Attitude Control System Using Integrating Gyros as Torque Sources. NASA TN D-1073, 1961.

4. DeLisle, J. E., Ogletree, G., and Hildebrandt, B. M.: Attitude Control of Satellites Using Integrating Gyroscopes. Instrumentation Lab., MIT Rep. R-350, 1961.

5. Ishlinski, A. Y.: Theory of the Double-Gyroscopic Vertical. NASA RE 3-10-59W, 1959.

6. Lopez, Armando E., Ratcliff, Jack W., and Havill, Jerry R.: Results of Studies on a Twin-Gyro Attitude Control System for Space Vehicles. AIAA Paper 63-332.

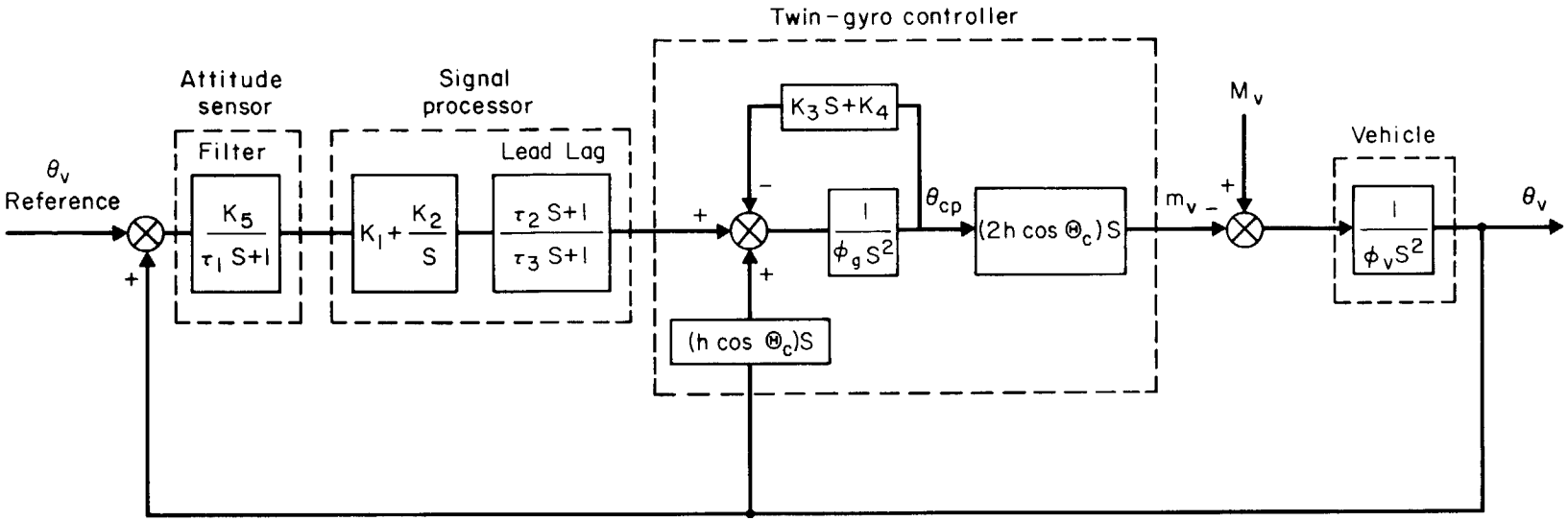

Figure 1.- Block diagram of a single-axis twin-gyro attitude control system.

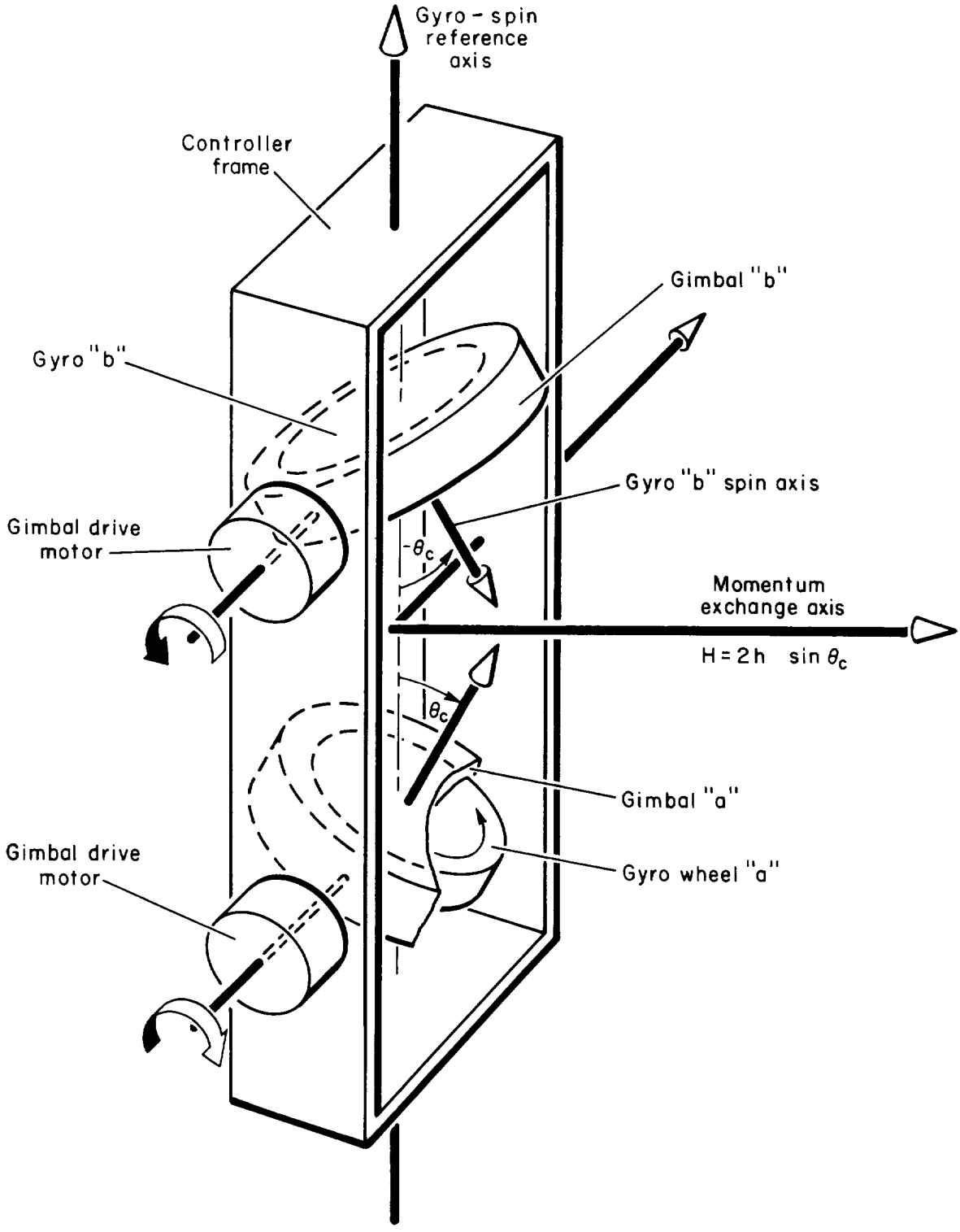

Figure 2.- Diagram of a twin-gyro controller.

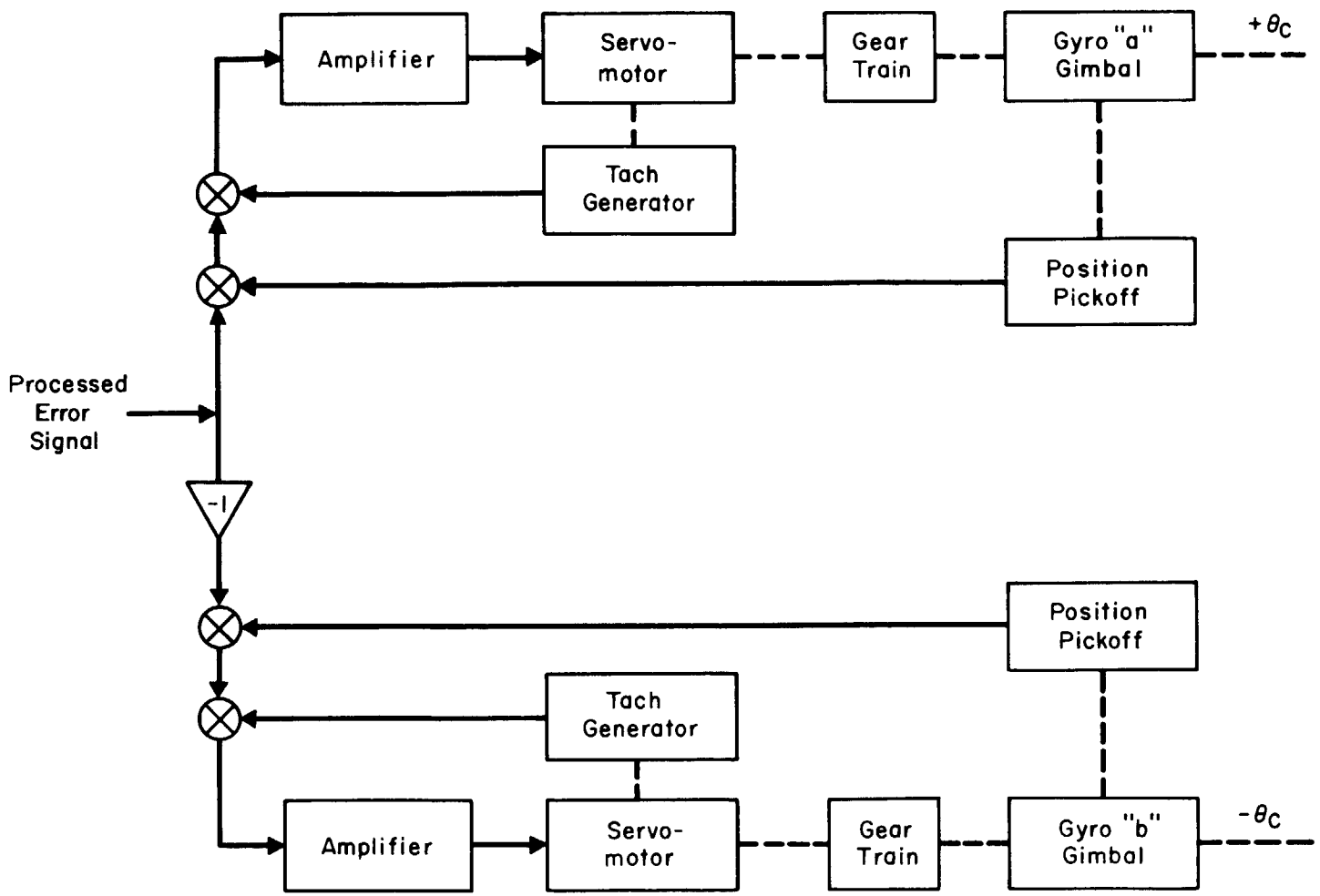

Figure 3.- Block diagram of single-axis twin-gyro controller.

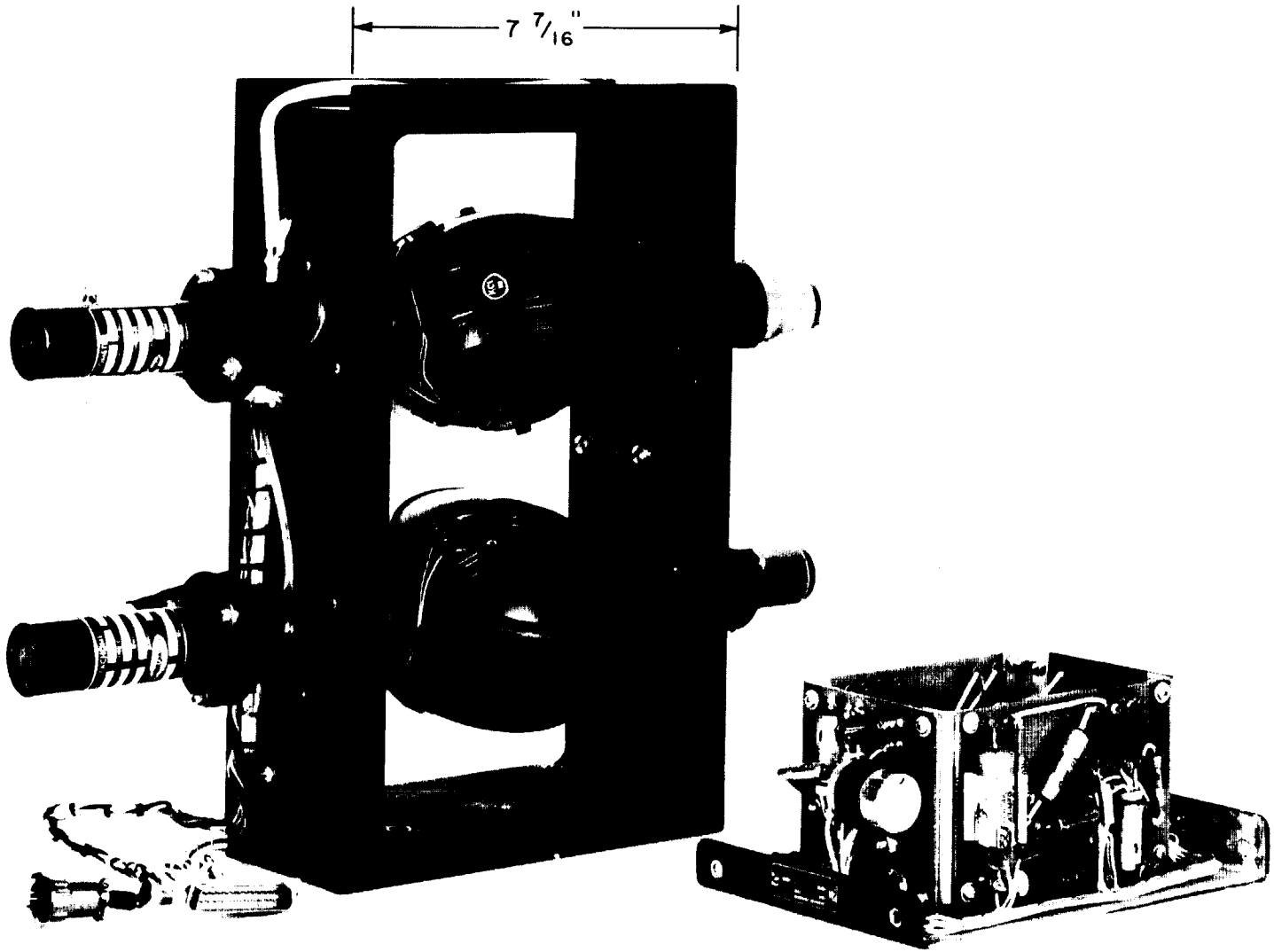

A-29648.3

Figure 4.- A single-axis twin-gyro controller.

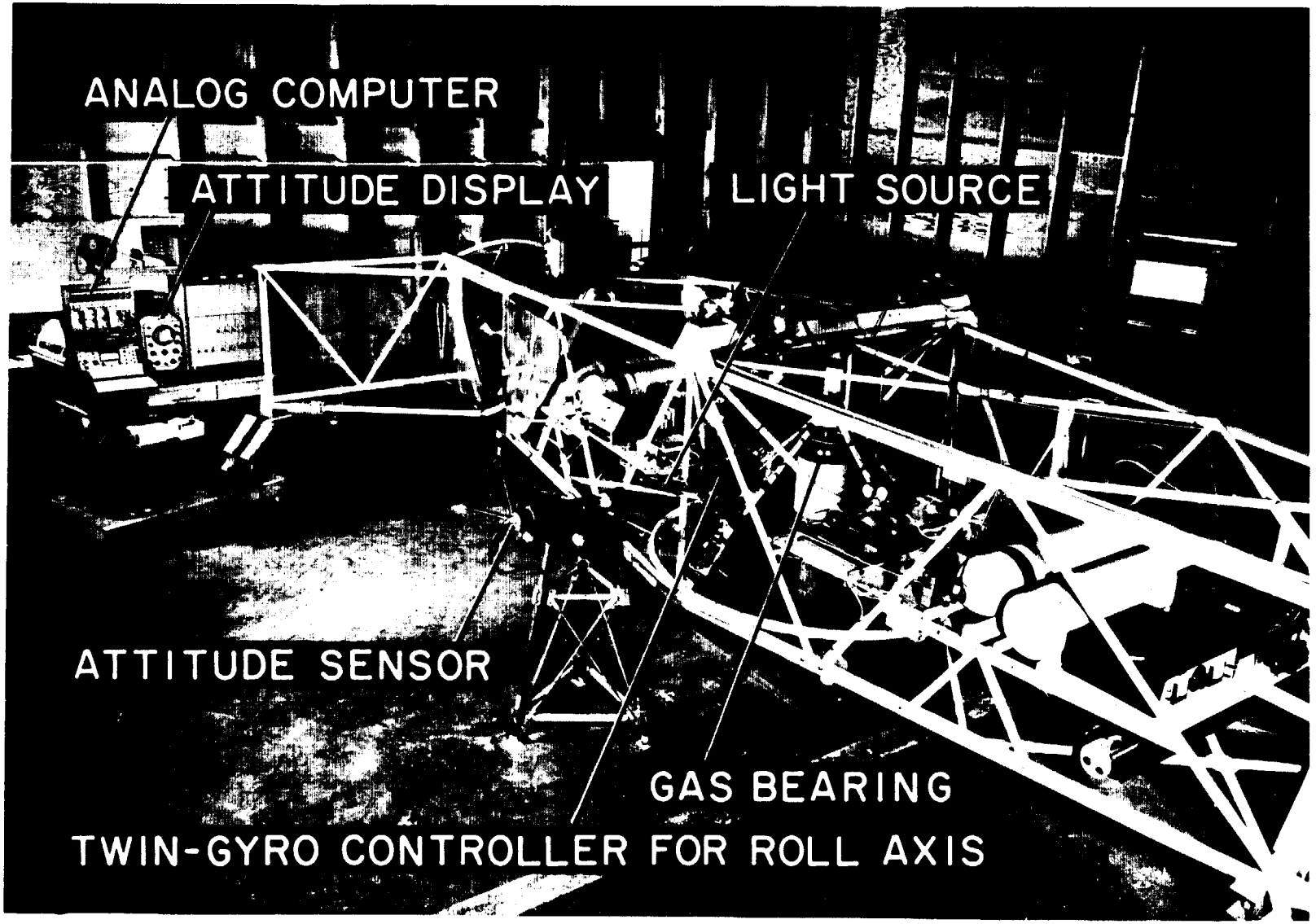

Figure 5.- Photograph of the space vehicle attitude simulator.

A-29934.2

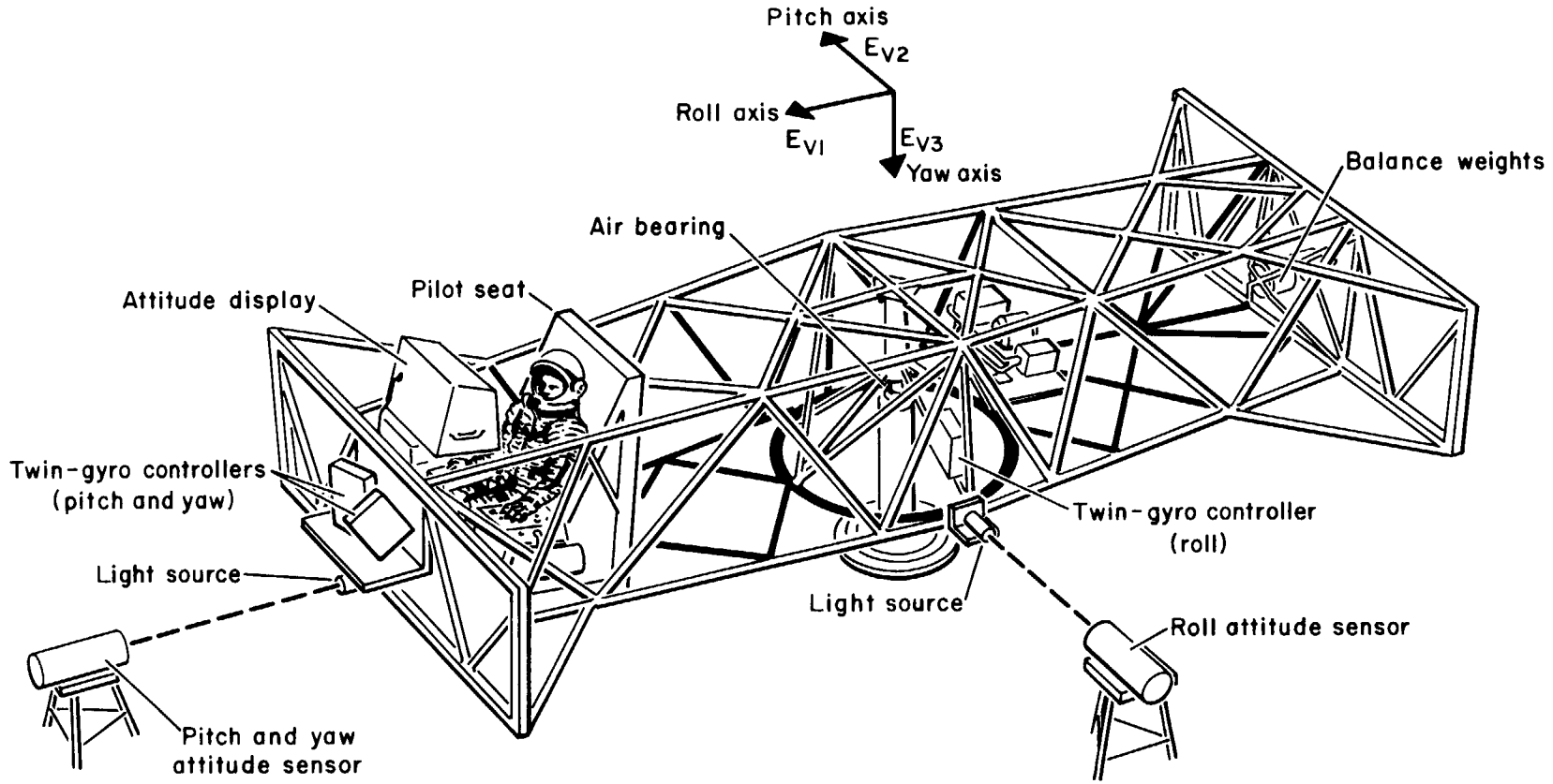

Figure 6.- Schematic view of space vehicle attitude simulator.

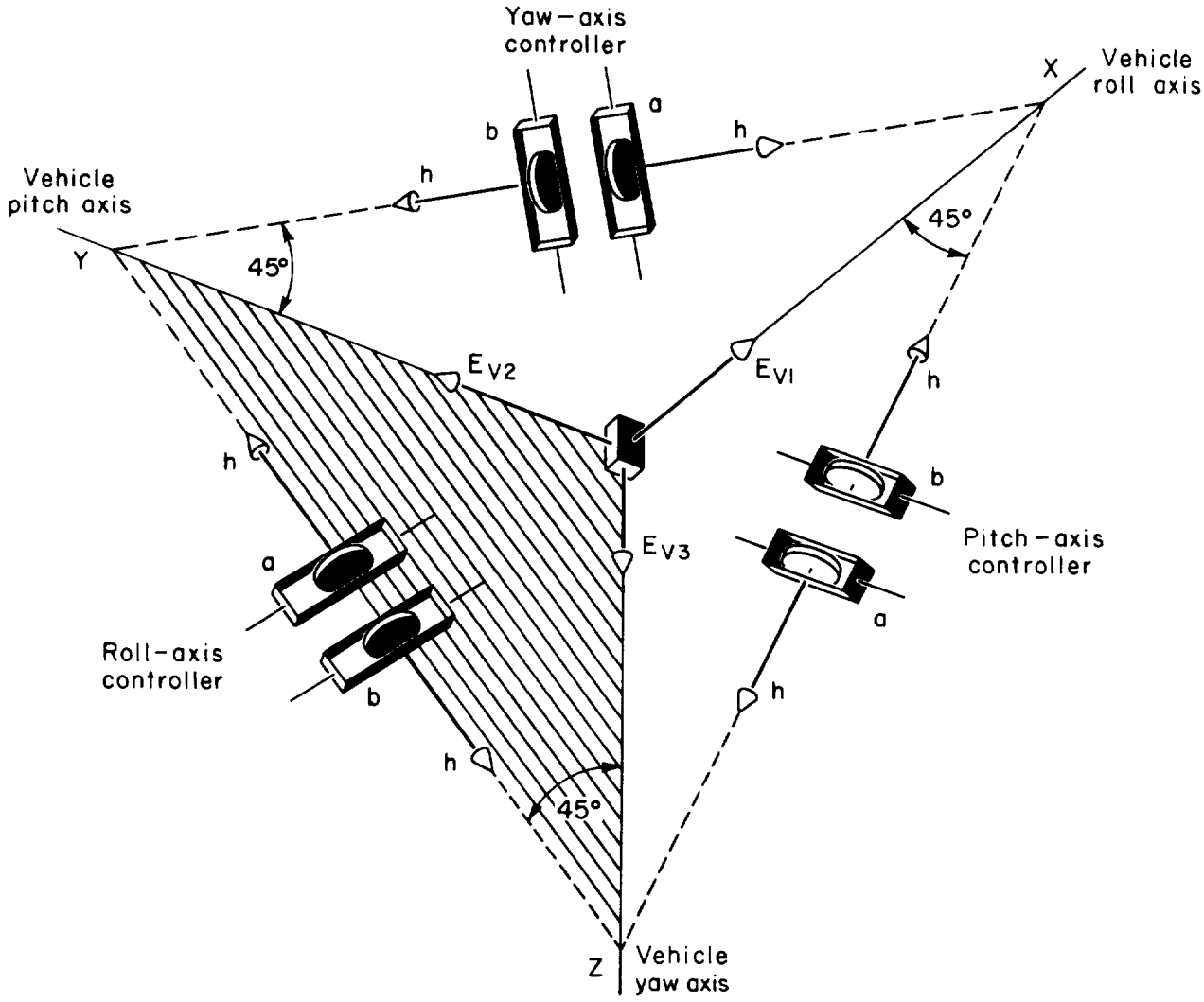

Figure 7.- Orientation of twin-gyro controllers with respect to the vehicle simulator.

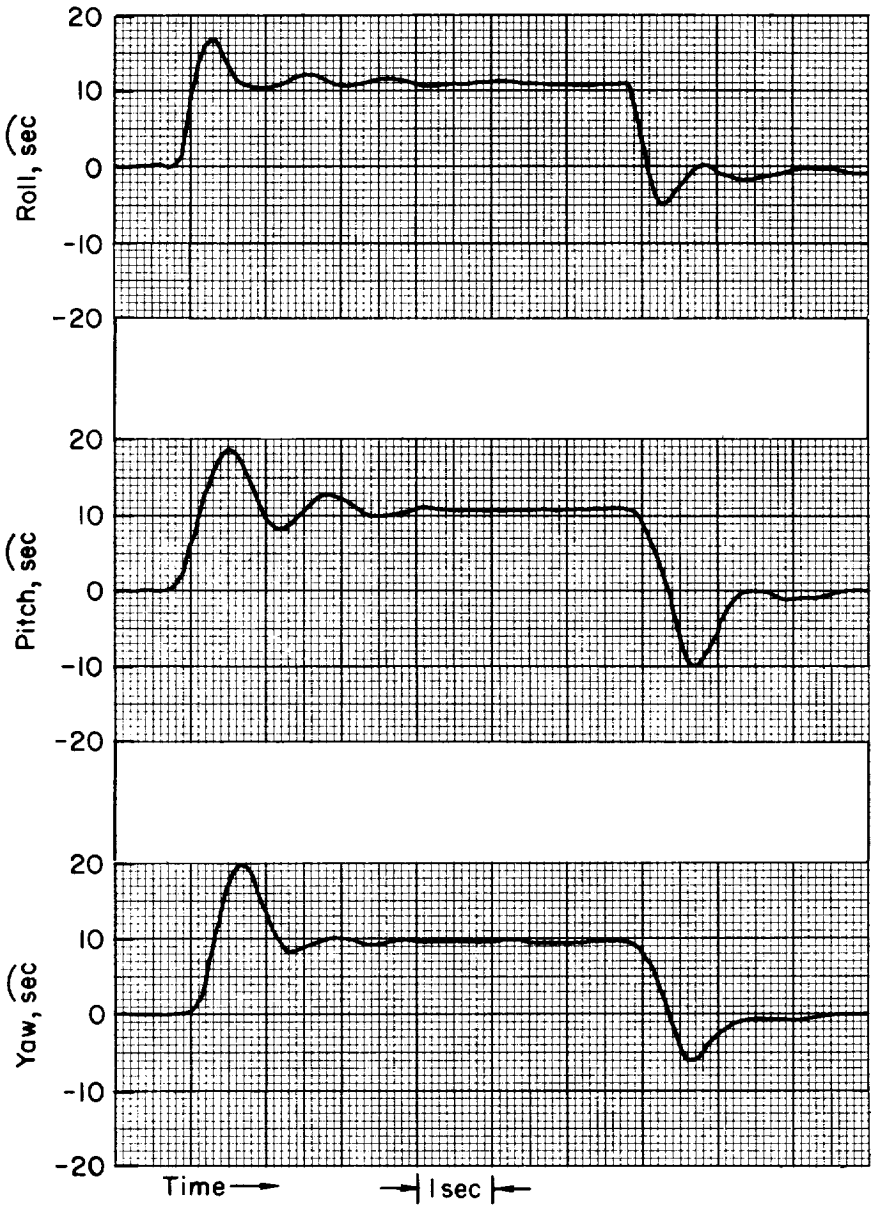

Figure 8.- Attitude response of simulator to simultaneous step input commands about all three axes.

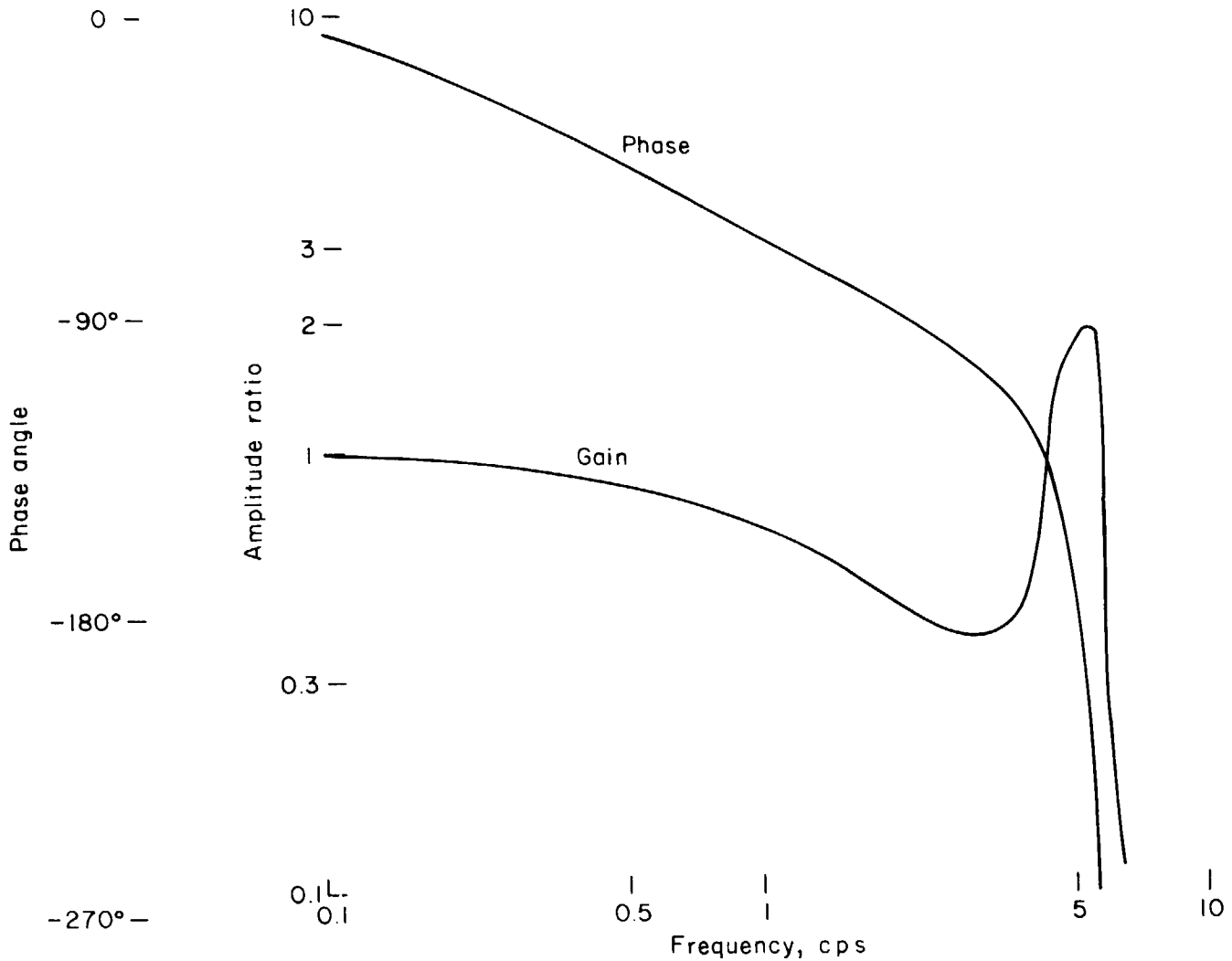

Figure 9.- Twin-gyro controller frequency response.

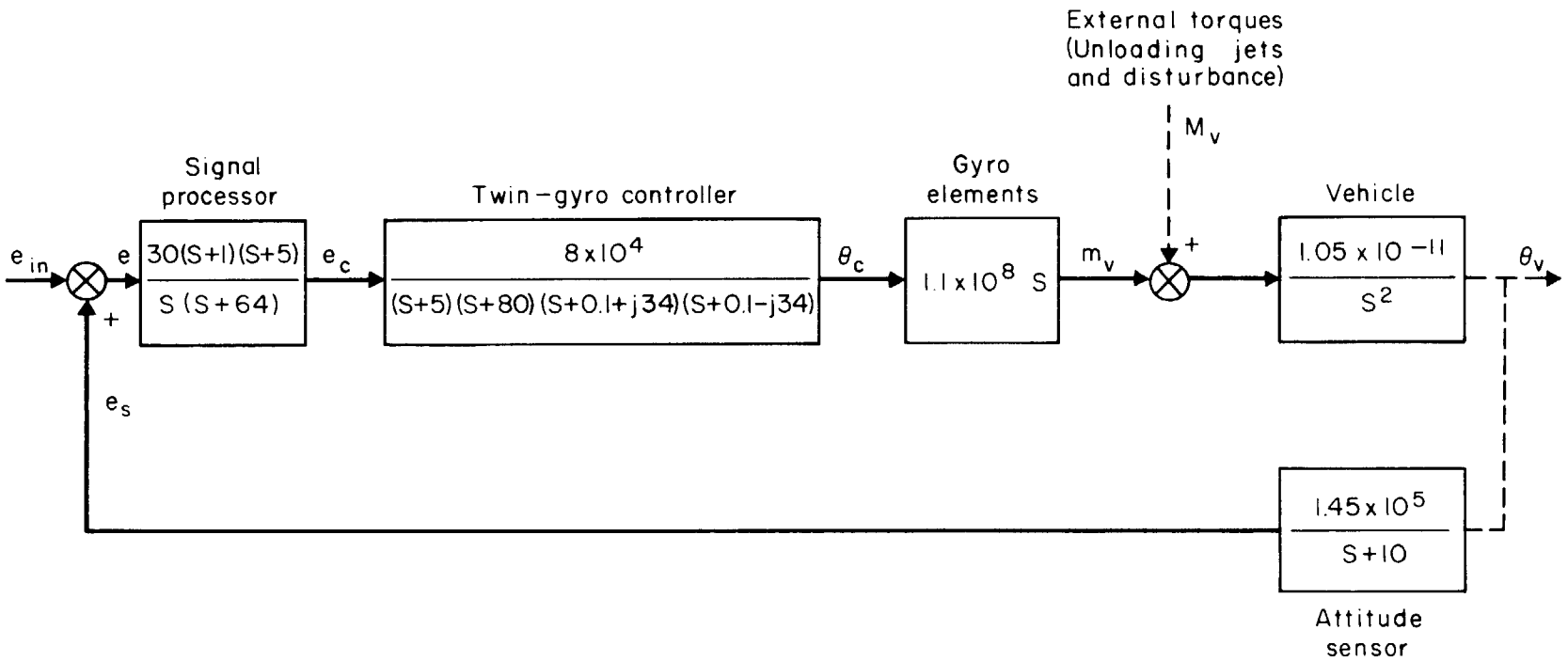

Figure 10.- Block diagram of yaw-axis transfer function.

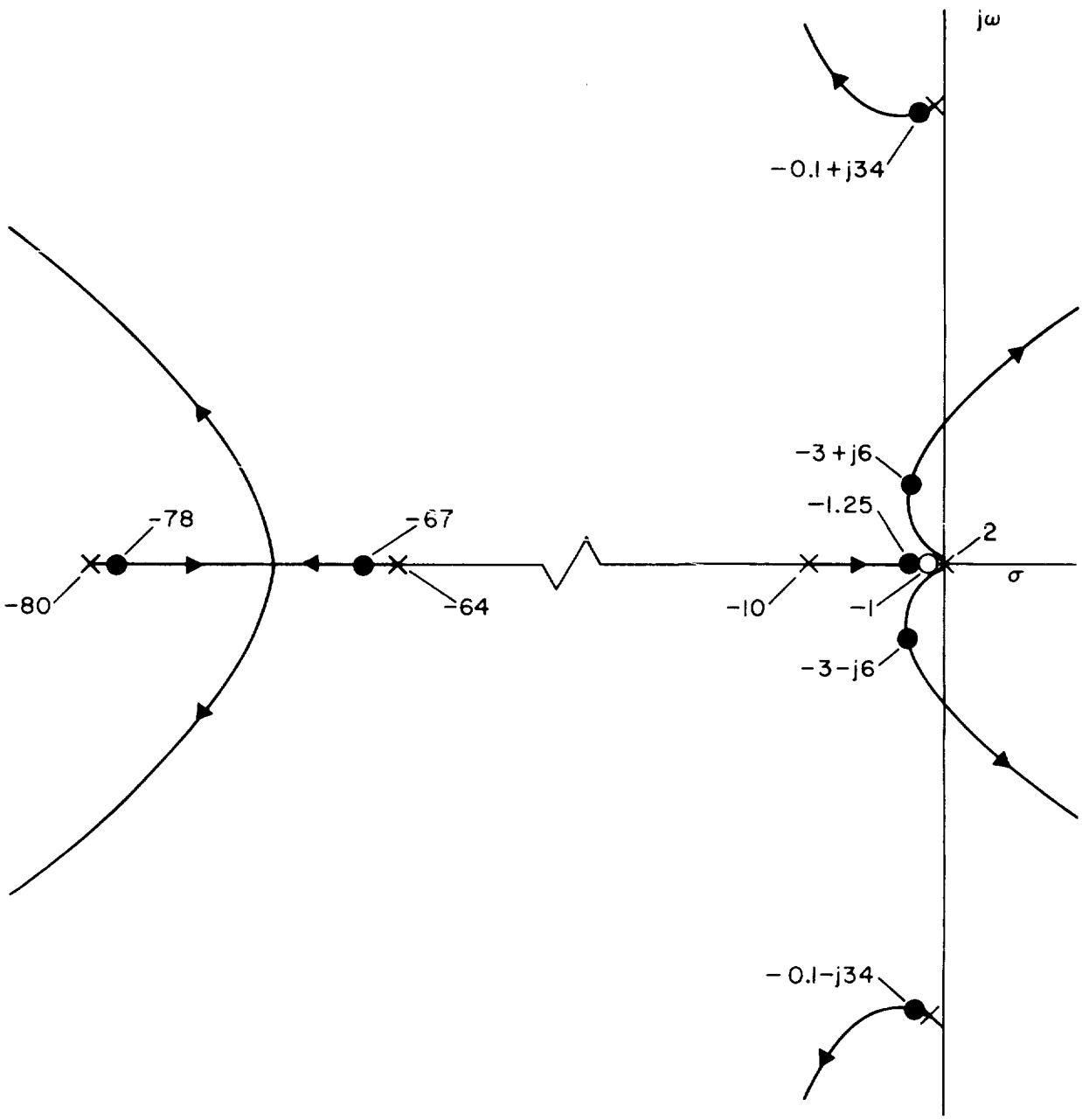

Figure 11.- Root locus of the characteristic equation of the control system.

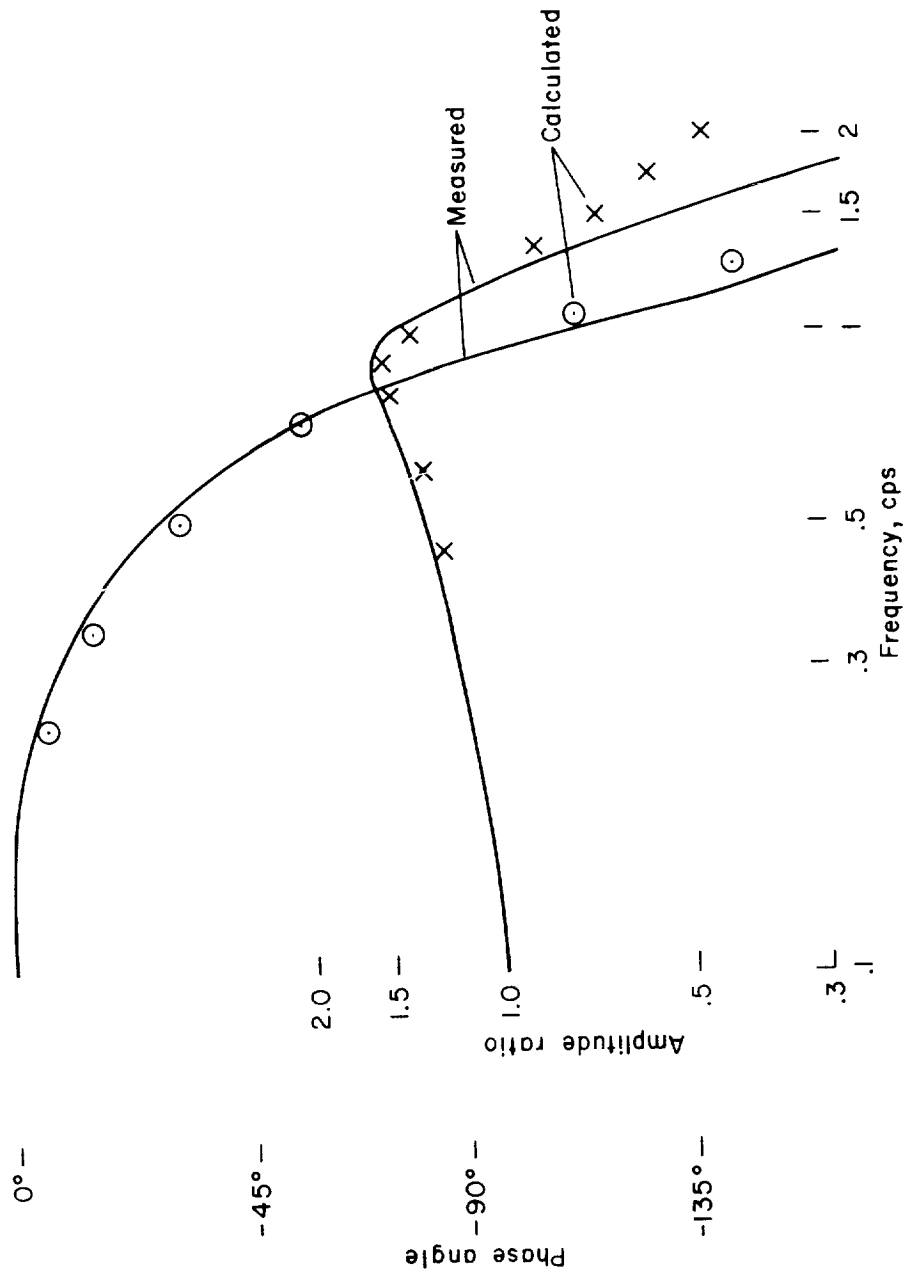

Figure 12.- Yaw-axis frequency response of vehicle simulator with twin-gyro control system.

NASA-Langley, 1964 A-651

NASA TN D-2419
National Aeronautics and Space Administration.
A TWIN-GYRO ATTITUDE CONTROL SYSTEM FOR SPACE VEHICLES. Jerry R. Havill and Jack W. Ratcliff. August 1964. 40p. OTS price, $1.00. (NASA TECHNICAL NOTE D-2419)

The twin-gyro controller described can transfer a major portion of the gyro momentum to the vehicle without inducing cross-coupling torques. A three-axis attitude control system is analyzed and tested experimentally on a space vehicle simulator. The data show that the system can stabilize a vehicle to precise attitudes with high dynamic response and that the response can be predicted analytically. Theoretical equations of motion are derived for a single-degree-of-freedom gyro, a twin-gyro controller, and a three-axis twin-gyro attitude control system.

I. Havill, Jerry R.
II. Ratcliff, Jack W.
III. NASA TN D-2419

NASA

NASA TN D-2419
National Aeronautics and Space Administration.
A TWIN-GYRO ATTITUDE CONTROL SYSTEM FOR SPACE VEHICLES. Jerry R. Havill and Jack W. Ratcliff. August 1964. 40p. OTS price, $1.00. (NASA TECHNICAL NOTE D-2419)

The twin-gyro controller described can transfer a major portion of the gyro momentum to the vehicle without inducing cross-coupling torques. A three-axis attitude control system is analyzed and tested experimentally on a space vehicle simulator. The data show that the system can stabilize a vehicle to precise attitudes with high dynamic response and that the response can be predicted analytically. Theoretical equations of motion are derived for a single-degree-of-freedom gyro, a twin-gyro controller, and a three-axis twin-gyro attitude control system.

I. Havill, Jerry R.
II. Ratcliff, Jack W.
III. NASA TN D-2419

NASA

NASA TN D-2419
National Aeronautics and Space Administration.
A TWIN-GYRO ATTITUDE CONTROL SYSTEM FOR SPACE VEHICLES. Jerry R. Havill and Jack W. Ratcliff. August 1964. 40p. OTS price, $1.00. (NASA TECHNICAL NOTE D-2419)

The twin-gyro controller described can transfer a major portion of the gyro momentum to the vehicle without inducing cross-coupling torques. A three-axis attitude control system is analyzed and tested experimentally on a space vehicle simulator. The data show that the system can stabilize a vehicle to precise attitudes with high dynamic response and that the response can be predicted analytically. Theoretical equations of motion are derived for a single-degree-of-freedom gyro, a twin-gyro controller, and a three-axis twin-gyro attitude control system.

I. Havill, Jerry R.
II. Ratcliff, Jack W.
III. NASA TN D-2419

NASA

NASA TN D-2419
National Aeronautics and Space Administration.
A TWIN-GYRO ATTITUDE CONTROL SYSTEM FOR SPACE VEHICLES. Jerry R. Havill and Jack W. Ratcliff. August 1964. 40p. OTS price, $1.00. (NASA TECHNICAL NOTE D-2419)

The twin-gyro controller described can transfer a major portion of the gyro momentum to the vehicle without inducing cross-coupling torques. A three-axis attitude control system is analyzed and tested experimentally on a space vehicle simulator. The data show that the system can stabilize a vehicle to precise attitudes with high dynamic response and that the response can be predicted analytically. Theoretical equations of motion are derived for a single-degree-of-freedom gyro, a twin-gyro controller, and a three-axis twin-gyro attitude control system.

I. Havill, Jerry R.
II. Ratcliff, Jack W.
III. NASA TN D-2419

NASA